Application of Micro-Nano Bubbles on Bioconversion of Carbon Dioxide and Hydrogen to Methane

July 2018

Liu Ye

Application of Micro-Nano Bubbles on Bioconversion of Carbon Dioxide and Hydrogen to Methane

A Dissertation Submitted to
the Graduate School of Life and Environmental Sciences,
University of Tsukuba
in Partial Fulfillment of the Requirements
for the Degree of Doctor of Philosophy in Environmental Studies
(Doctoral Program in Sustainable Environmental Studies)

Liu Ye

Abstract

The conversion of CO_2 to other valuable carbonic compound is one of the effective way to alleviate the greenhouse effect in the world. Unlike the chemical procedure, which employs the costly catalysts, such as Ru, Pb, Rh, etc, under the high pressure or temperature condition, the bioconversion of CO_2 by hydrogenotrophic methanogens can realize the transformation from CO_2 to biofuel (CH_4) under a mild condition with a lower cost. However, the mass transfer of hydrogen, and the low biomass growth rate remain as the hurdles for this procedure. However, the low gas-liquid mass transfer (k_La) of H_2 limits the commercial application of this bioconversion. Micro-nano bubbles (MNBs) are tiny bubbles with diameters ranging from tens of nanometers to several tens of micrometers. MNBs had been widely used in various medical, wastewater purification, food processing, marine and agriculture applications. Several special characteristics of MNBs, such as high specific area (surface area per volume) and high stagnation in liquid phase, increase the gas dissolution. Moreover, it has been reported that the collapse of micro-bubbles, due to the high density of ions in gas-liquid interface just before the collapse, will lead to free radical generation, which might be favorable for microbial metabolism and further stimulate the bioactivity. Up to now, however, little information can be found on the combination of MNB with anaerobic microorganisms.

The objectives of this study are: 1) to apply the MNBs for bioconversion of H_2 and CO_2 to CH_4, to realize simultaneously CO_2 removal with renewable biofuel production, and 2) to investigate the feasibility and mechanism of enhancement for methane yield, and finally 3) to promote the large-scale application of MNBs by conducting the influencing factors experiments to find the optimal conditions.

Firstly, this study explored the feasibility of applying the micro-nano bubbles for bioconversion by constructing two stirred tank reactors (STRs) equipped with a micro-nano sparger (MNS) and common micro sparger (CMS), respectively. MNS was found to display superiority to CMS in methane production with the maximum methane evolution rate (MER) of 171.40 mmol/L_R/d and 136.10 mmol/L_R/d, along with a specific biomass growth rate of 0.15 d^{-1} and 0.09 d^{-1}, respectively. The gas-liquid mass transfer of H_2 was twice in the MNSR (12.95 h^{-1}) compared with CMSR (6.60 h^{-1}) mainly due to the increased specific surface area. Energy analysis indicated that the energy-productivity ratio for MNS was higher than that for CMS.

Secondly, the effect of nano scale bubbles (NBs) on the bioconversion was investigated by preparing liquid medium with or without H_2/CO_2 mixture nano bubbles. The results showed

that both methane production and VFAs degradation were enhanced by the pre-supplementation of NBs in the liquid. The higher coenzyme F_{420} content was obtained in the inoculated nano bubble medium (INBM) group with content of 1.84 μmol/g-VS, while 1.56 μmol/g-VS for inoculated distilled medium (IDM) group. The intracellular Fe contents in INBM group were higher than the distilled water (DW) group, with the concentration of 1159.53±20.34, 1035.28±12.01 μg/g-VS, respectively. For the metal speciation, the higher percentage of acid soluble and exchangeable fraction, while lower percentage of organic matter and sulfide fractions in the NBW group were achieved than the DW group. The micro-nano bubbles may enhanced the mass transfer and bioavailability of trace metals.

Thirdly, the effect of air NBs on bioconversion was investigated under different initial iron and cysteine concentrations. Results showed that for the inoculated groups, the stimulation for methane production by air NBs was more obvious under lower iron (50 μM) or cysteine concentrations (3 mM). The methane production was inhibited at 100 μM Fe concentration, while the more obvious inhibition was obtained in NB group. The soluble sulfide concentration increased for all the nano bubble groups compared with the groups without bubbles, especially under 6 mM cysteine concentration (0.62 mg/L in NB group, 0,42 mg/L in control group). For the pure medium, the bubbles may combine with the particles, which can be proved by an increased zeta potential (from -31.80±1.90 to -26.62±2.05). While the ORP before and after introduction of NBs did not change obviously. For the metal speciation analysis, the increase in Fe concentrations lead to an increase in adsorbed fractions, and the existence of NBs enhanced this increment.

This study provided a possible application of micro-nano bubbles for bioconversion of CO_2 to CH_4. Enhanced mass transfer of H_2 and biomass growth, while low energy consumption were obtained, suggesting that MNS can be used as an applicable resolution to the limited k_La of H_2 and thus enhance the bioconversion. The existence of nano bubbles may improve the bioavailability and mass transfer of trace metals. Based on these results, the micro-nano bubble aeration may be a potential pre-treatment for improving the microbial activity and bioconversion efficiency.

Keywords: Micro-nano bubbles, hydrogenotrophic methanogens, mass transfer, Bioavailability.

Contents

List of tables

List of figures

Abbreviations

CMS	Common micro sparger
CMSR	Reactor with common micro sparger
CSTR	Continuously stirred tank reactor
DM	Medium without nano bubbles
DW	Distilled water
IDM	Isolated medium without nano bubbles
INBM	Isolated medium with nano bubbles
MNBs	Micro-nano bubbles
MNS	Micro-nano sparger
MNSR	Reactor with micro-nano sparger
NBs	Nano bubbles
NBM	Medium with nano bubbles
NBW	Distilled water with nano bubbles
PBR	Packed bed reactor
STR	Stirred tank reactor
TBR	Trickle bed reactor
UASB	Upflow anaerobic sludge blanket
UBF	Upflow blanket filter

Chapter 1 Introduction

1.1 Bioconversion of CO_2 to CH_4

1.1.1 Hydrogenotrophic methanogens

Methanogens can be classified into three types according to different substrates utilization, acetoclastic methanogens, methanol methanogens and hydrogenotrophic methanogens. Hydrogenotrophic methanogens utilize CO_2 and H_2, as carbon and energy source, respectively, to realize simultaneous growth and CH_4 production (Thauer et al., 2008). The characteristics of CO_2-type hydrogenotrophic methanogens has been elucidated by many extraordinary studies (Rospert et al., 1990, 1991; Bonacker et al., 1993; Deppenmeier, 2002). In comparison to the chemical-based methanogenesis process (Satier process), bio-conversion offers many benefits including the relatively moderate condition with the temperature range of -5 ℃ to 122 ℃ (Cavicchioli, 2011), much lower than the range for chemical conversion (250 ℃ to 400 ℃) (Hoekman et al., 2009). The methanogens employ the inexpensive elements like nickel and iron as the catalysts for the bioreactions (Liu & Whitman, 2008), instead of the costly materials (ruthenium and titan) (Brooks et al., 2007).

In order to realize the bioconversion of CO_2 to methane, the reduction by H_2 is of special interest. Currently, H_2 can be produced from renewable energy (i.e. wind or solar power) via water electrolysis (Hoekman et al., 2009) or obtained from biological process (biohydrogen) (Benemann, 2000; Ghirardi et al., 2000; Redwood & Macaskie, 2006; Redwood et al., 2012; Rittamann & Herwig, 2012). H_2 is also contained in waste gas emitted from the industry (de Filippis et al., 2004). This emphasizes bioconversion of CO_2 to CH_4 as a highly promising bioprocess for simultaneous CO_2 capture and energy conversion and storage.

1.1.2 Limitation of bioconversion

However, the main barrier for the commercial scale-up of the bioconversion is the gas-liquid mass transfer of H_2, due to its low solubility. Bioconversion of CO_2 to CH_4 is a heterogeneous system consisting of gaseous substrate, liquid fermentation medium and solid cells. Generally, the conversion rates are limited by the gas-liquid mass transfer in the bioprocesses which use sparingly soluble gases as key substrates. For instance, homoacetogens utilize CO or H_2 as carbon and energy sources, while, aerobic respiration employs O_2 as electron acceptors for ATP generation (Rittmann et al., 2015). Vega et al. (1989) summarized that gas to liquid mass transfer phenomenon consist of multiple steps, (I) the absorption of a gaseous

substrate across the gas-liquid interface, (II) the transfer of the dissolved gas to the fermentation media and (III) diffusion through the culture media to the cell surface. Compared with the other limitation factors for the mass transfer, including the properties of the liquid, mixing rate, bubble size, interfacial adsorption, etc., the solubility of gaseous substrates (sparingly soluble) in the biochemical reaction is the biggest obstacle to the mass transfer (Klasson et al., 1992; Munasinghe and Khanal, 2010; Vega et al., 1989).

1.1.3 Solutions to overcome gas-liquid mass transfer limitation

Higher productivities of a bioprocess are strongly dependent on the high mass transfer rate and high cell concentration (Liu et al., 2014). The results of Chang et al. (2001) showed that the poor mass transfer of gaseous substrates led to the low cell, indicating that the gas-liquid mass transfer was the most limiting factor in the fermentation reaction, leading to reduced productivity. Most of these methods depend on increasing the interfacial surface area and promote the bubble breakup by increasing the agitator's mixing rate. However, these approaches are energy and cost intensive and hard to be scaled up. To simultaneously realize the energy efficiency and high mass transferred conditions, different bioreactor configurations have been investigated for maximum bioconversion. Researchers obtained the efficiency of mass transfer rate in these reactors by predicting the k_La according to the hydrodynamic conditions (Munasinghe and Khanal, 2010).

The mass transfer of O_2 is also a critical parameter for aerobic bioreactor development. However, the difference is that oxygen is just partially converted because of the excess supply of oxygen in the aerobic processes, bioconversion of CO_2 focuses at full conversion of the gaseous substrates even at high H_2/CO_2 gassing rates. This is a much critical demand for bioreactor design since when considering the suitable methods for enhancement of mass transfer in aerobic cultures, the possible decrease in biological conversion efficiency of CO_2 can not be neglected. Many researchers focused on investigating and optimizing the gas-liquid mass transfer by bioreactor design. The most widely used bioreactor was continuously stirred tank reactor (CSTR) (de Poorter et al., 2007; Nishimura et al., 1992; Peillex et al., 1990; Rittmann et al., 2012; Schoenheit et al., 1980). Other methods were also employed for improving the mass transfer of hydrogen as shown in Table 1-1.

1.2 Micro-nano bubbles

Recently, many researchers utilized the ultrafine bubbles including microbubbles (MBs)

and nanobubbles (NBs) to improve the gas-liquid mass transfer of sparingly soluble gases. Most studies focused on the fundamental researches, such as generation methods, measuring techniques, and characterization of the fine bubbles. Whereas few studies revealed the feasibility of micro-nano bubbles for scaling up application at commercial levels. Johnson and Cooke (1981) reported the earliest direct evidence of bulk nanobubbles with diameters of < 1 μm. They reported that bubbles produced can survive for long periods (about 22 h) as a result of the formation of surface films assistant by naturally present surfactants. They demonstrated the bubbles may expanded when under negative pressure and shrank by applying the applied pressure because they are gas-filled.

1.2.1 Definition and classification of micro-nano bubbles

Bubbles were classified based on different characteristics, including bubble size, surface nature, and the lifetime of the bubbles. Ushikubo et al. (2010) found that bubbles size distribution decided most of these factors. Hence, the bubble size was the most frequently used classification basis. Accordingly, various studies defined the bubbles as macro bubbles, micro bubbles, and sub-micro or nano bubbles for conventional or big bubbles, fine bubbles, and ultrafine bubbles, respectively. Nano bubbles consist of the surface nanobubbles and bulk nanobubbles. Surface nano bubbles existed on a surface, are in the form of a spherical cap, with the diameter of 10-100 nm. While, the bulk nano bubbles are spherical bubbles with the diameter of < 1000 nm. The alternative term for nano bubbles is ultrafine bubbles.

1.2.2 Characteristics of MNBs

(1) Slow rising rate

According to the description of Li et al. (2014), Stokes' law could be applied for the calculation of the rising velocity of micro-nano bubbles. It can be found that the size of radius is in proportion to the rising speed. Takahashi et al. (2009) pointed out that the rising velocity of microbubbles bigger than 7-8 μm approximately obeyed the Stokes' law, while the rising speed of smaller bubbles was more slowly than calculated. The evolution procedure for different size bubbles was shown in Fig. 1-1.

(2) High pressure inside MBs

As shown in Young-Laplace equation (Eq. (1-1)), the surface tension σ may lead to the increase in the inside pressure of a bubble (ΔP) with diameter (d), even larger than the surrounding environment.

$\Delta P = 4\sigma/d$ (1-1)

The pressure in the bubble increases with the decrease in bubble size. When decreasing bubble size, the partial pressure of gas component inside the bubbles increases, accordingly, the gas dissolves easily.

(3) Large interfacial area

Eq. (1-2) showed the interfacial area. Smaller bubble diameter d is beneficial to the interfacial area (A/V) and gas dissolution fraction.

$A/V = 6/d$ (1-2)

(4) Large gas dissolution

If the gas phase mass transfer resistance can be neglected, Eq. (1-3) can be utilized to calculate the gas-liquid mass transfer rate, or the dissolving rate N (mol/s).

$N = k_L a(p - p^*)/H$ (1-3)

where k_L is the liquid phase mass transfer coefficient (m/s), a is the bubble surface area (m^2), p is the partial pressure of dissolved component in bubble (Pa), p^* is the partial pressure of gas phase equilibrium with dissolved component in liquid (Pa) and H is the Henry constant.

k_L is written by Eq. (1-4), and the rising velocity of spherical bubble follows Stokes' law, where D_L is the gas diffusion coefficient in liquid phase, and U is the bubble rising velocity.

$$k_L = \frac{D_L}{d}\left[1 + \left(1 + \frac{dU}{D_L}\right)^{1/3}\right] \quad (1\text{-}4)$$

When a bigger bubble (1 mm) shrinks into smaller bubbles with the diameters of 10 μm and 100 nm, the numbers increase by 106 and 1012 times, respectively, therefore, the surface areas increase by 6×10^4 and 6×10^{10} folds, respectively. By using MNBs, the dissolution rate increases rapidly.

(5) Electrostatically charged surface

The MNBs are usually surface charged and the electrical property depends on the relationship between pH and their isoelectric point. Consequently, the repulsion force may formed between the MNBs.

(6) Longer retention time

The stabilization of nano-bubbles in water was investigated by Ushikubo et al. (2010) by measuring the particle size distribution, zeta potential and proton NMR spin-lattice relaxation

time. Results showed that the oxygen nano-bubbles survived for several days. NMR spin-lattice relaxation time increased with the existence of micro-nano bubbles. The stability of nano-bubbles may be caused by the electrically surface charge which makes the bubbles repulse with each other, further prevent the coalescence. The lifetime of a bubble can be obtained by employing Eq. (1-5) proposed by Ljunggren et al. (1997).

$$t = \frac{K{d_0}^2}{12RTD} \tag{1-5}$$

where K, d_0, R, T, and D are the Henry law constant, bubble diameter at t= 0, gas constant, temperature, and diffusion constant, respectively. Based on the assumption of Tsuge et al. (2014), the lifespan of bulk NBs is about 0.41 μs, and the concentration of bulk NB will not increase with the mixing time.

1.2.3 Application of MNBs

(1) In physicochemical field

1) Flotation

Flotation is one of the traditional approaches to separate the solid from water, including powders, chemicals, metal ions, oils and organics (Rubio et al., 2002). The decrease in bubble size is beneficial to the flotation efficiency. Accordingly, micro-nano bubbles were utilized to the flotation processes (Miettinen et al., 2010). Yoon et al. (1993) reported bubble size reduction may providing higher probability for the collusion of small particles with fine gangue. The similar size and opposite charge between the MNBs and the fine particles lead to more chance of collision and make the flotation much easier (Haarhoff et al., 2001). Fan et al. (2010) showed that the presence of NB broadened flotation particle size range and increased particle surface hydrophobicity. Moreover, from the economic aspect, the NB flotation technology followed by coagulation/flocculation is found to be cost-effective than the conventional processes. While, the feasibility of the NB flotation for a field scale application still need to be explored further.

2) Advanced oxidation

Advanced oxidation process is another most common technology utilizing the bubbles. The main objectives of applying MNBs technologies are to improve the solubility of ozone, which can further enhance the oxidation efficiency and realize the high removal efficiency with low energy and cost consumption.

(2) In biological field

The MNBs were also applied in the biological field for enhancing the biological matter degradation, microbial growth rate, seed germination, and growth rates.

1) Application for animals

In the 1980s, microbubble generators was introduced to aquaculture, such as shellfish and fish culture, aiming at relieving the shortage of oxygen supply due to high-density culturing. Endo et al. (2008) using a microbubble generator to create the rotational flow to control the DO levels, which had a prominent advantage to treat a large amount of the water in the fish farms due to the excellent ability of controlling DO levels and the low energy consumption compared to the conventional aeration devices.

Ebina et al. (2013) investigated the effect of the NB aeration on the growth of fish and mice. Results showed that Total weight of sweetfish increased from 3.0 to 6.4 kg in normal water, whereas it increased from 3.0 to 10.2 kg in air-nanobubble water. Free oral intake of oxygen-nanobubble water significantly promoted the weight (23.5 vs. 21.8 g; *p*, 0.01) and the length (17.0 vs. 16.1 cm; *p*, 0.001) of mice compared to that of normal water. Researches revealed that oxygen-rich water brought about by micro/nano bubble injection enhances blood flow and branchial respiration of fishes. Some researchers utilized the nitrogen nanobubbles to create an ultra-low oxygen condition to keep fishes fresh. Under such conditions freshness is successfully kept at least 8 days with good taste. Similarly, the CO_2 nano bubbles were utilized as a media for keeping fishes asleep to meet the requirements of long distance transport. The high dissolubility of gases induced by micro-nano bubbles contributed mostly to all of applications in the animals fields.

2) Application for plants

Ebina et al. (2013) explored the effect of nanobubbles on the growth of leaf lettuce (Lactuca satuva). Results showed that both the fresh (2.1 times) and dry weights (1.7 times) of the lettuce were improved with the aeration of NBs than that with the macro bubbles. Moreover, the germination rates of barley seeds dipped in nitrogen NB water was increased by 15-25 percentage than those dipped in distilled water, which indicated the significant effect of NBs on the physiological activity of plants. The mechanism with which nanobubbles (NBs) promote physiological activity was investigated using nuclear magnetic resonance (NMR) relaxation-time (T_2) measurements. The NB water showed a longer T_2 value than control water. While, the T_2 value of NB water decreased after degassing, indicating that the existence of NBs may lead to the difference of T_2 value. Liu et al. (2016) explored the oxygen NBs effect on germination of spinach and carrot seeds. The final germination rates of spinach seeds in distilled water, low-

number density NB water, and high-number density NB water were 54%, 65%, and 69%, respectively. The existence of NBs can also promote the growth of sprout growth. While the high density of NB water showed a negative effect on the carrot seeds, which was concluded by the authors that the amount of exogenous ·OH in high-number density NB water may do harm to hypocotyl elongation and chlorophyll formation. This study proposed that NB water may produce the exogenous reactive oxygen species (ROS) when NB collapse and provided a reasonable explanation for the promotion effects of oxygen NBs.

3) Application for aerobic microorganisms

Aeration is the effective method to provide the life-sustaining gas (O_2) to the aquatic lives and biochemical reactions for aerobic processes. The aerobic biological matter degradation and the growth of microbes can be improved by enhancing the aeration efficiency. Recently, MNBs were employed improve mass transfer in the area of aeration. Li et al. (2014) studied the dispersion and gas-liquid mass-transfer rate of oxygen. The organic waste degradation in the NB aerated unit was significantly shortened the retention time compared with the conventional system. Similarly, the biomass growth was enhanced with the existence of NBs. Wang et al. (2017) applied fine bubble aeration technology to a filtration system with aiming at treating the subsurface wastewater. The results show that fine bubble aeration can improve the effectiveness of nitrogen degradation. The effect of the fine bubble aeration technology is beneficial when it is used to strengthen land-treatment technology. However, the effect of MNBs on nitrifying bacteria and the other bacteria was overlooked. The results of Li et al. (2014) indicated the MNBs existed in the pore water may not significantly influence the hydraulic conductivity of the sand.

Ozonation is a promising method for disinfection of pathogens (Khuntia et al., 2015). The application of MNBs exhibited a faster reduction rate, a smaller tank size, and a lower ozone requirement in relation to the conventional ozonation process. The inactivation of E. coli was attributed to the generation of ·OH and shock waves from collapsing MBs. In addition, the MNBs may lead to higher mass transfer of ozone, resulting in a higher dissolved ozone and ·OH amount, which was benefit for improving the disinfection efficiency.

While, there are still no studies focused on the effect of MNBs for the anaerobic microorganisms. So that this study intends to investigate the variation of anaerobic microorganisms with the existence of MNBs.

1.3 The originality and contents of this study

1.3.1 The originality and objectives

The aims of this study are:

1) To investigate the effect of MNBs for the anaerobic microbe, hydrogenotrophic methanogens. Try to reveal whether the MNBs will enhance the bioconversion of CO_2 and H_2 to CH_4 or not.
2) To explore the mechanism for the effect induced by the MNBs. In other words, to reveal how the MNBs affect the anaerobic procedure.
3) To identify the effect of MNBs under different conditions. In this study, the trace metal concentration and sulfur source concentration were chosen as the influencing factors, to investigate the bioconversion proformance with or without nano bubbles under different level of trace metal and sulfur concentrations.

1.3.2 The contents of this study

The summary of the contents of this study were drawn in Fig. 1-2.

In the first experiment, two stirring tank reactors were constructed with different spargers (a common micro sparger & a micro-nano sparger) to supply the H_2/CO_2 mixture for the methanogens continuously. Further decreased the bubble size leads to the higher solubility of the hydrogen. Based on this, the methane production, VFAs variation and biomass enrichment were analyzed. The gas-liquid mass transfer of hydrogen was also measured. After analyzing the performance for the two systems, the energy consumption was also investigated.

In the second experiment, the H_2/CO_2 mixture nano bubbles were pre-loaded to the medium. The medium without nano bubble introduction was set as the control group. Under conditions with or without nano bubbles, CH_4 and VFAs were analyzed. The coenzyme F_{420} were measured to reveal the microbial activity. Cause the trace metal elements were the key components for coenzyme synthesis, the trace metal content in the cells were also detected. The metal speciation helps us to understand the variation of different fractions of metal with time.

In the third experiment, instead of H_2/CO_2 mixture, air was chosen as the gas source for the generation of nano bubbles. Oxygen was one of the main component of air, while it is harmful for the anaerobic processes. Therefore, whether the air nano bubbles will benefit or harm the bioconversion to methane need to be explored. What's more, how the effect will be influenced by the variation of conditions favor to the larger scale application of micro nano bubbles. The iron concentration and initial cysteine concentration were set as the indicators for

the condition variation. And also to confirm the accuracy of mechanism investigated in the second experiment by conducting the experiments under different conditions.

Table 1-1 Summary of solutions for improving the gas-liquid mass transfer of hydrogen.

Methods	References
Increasing agitation speed	Robinson and Wilke, 1973; Kramer and Bailey, 1991; Luo et al., 2013
Gas or liquid flow rate	Guiot et al., 2011; Yagi and Yoshida, 1975
Reactor geometry (CSTR, TBR, PBR)	Klasson et al., 1992; Jee et al., 1988a; Luo & Angelidaki, 2013
Nature of liquid (surfactant)	Bredwell et al., 1997
Increasing the specific surface area (microbubble sparger)	Bredwell et al., 1999; Munasinghe and Khanal, 2012

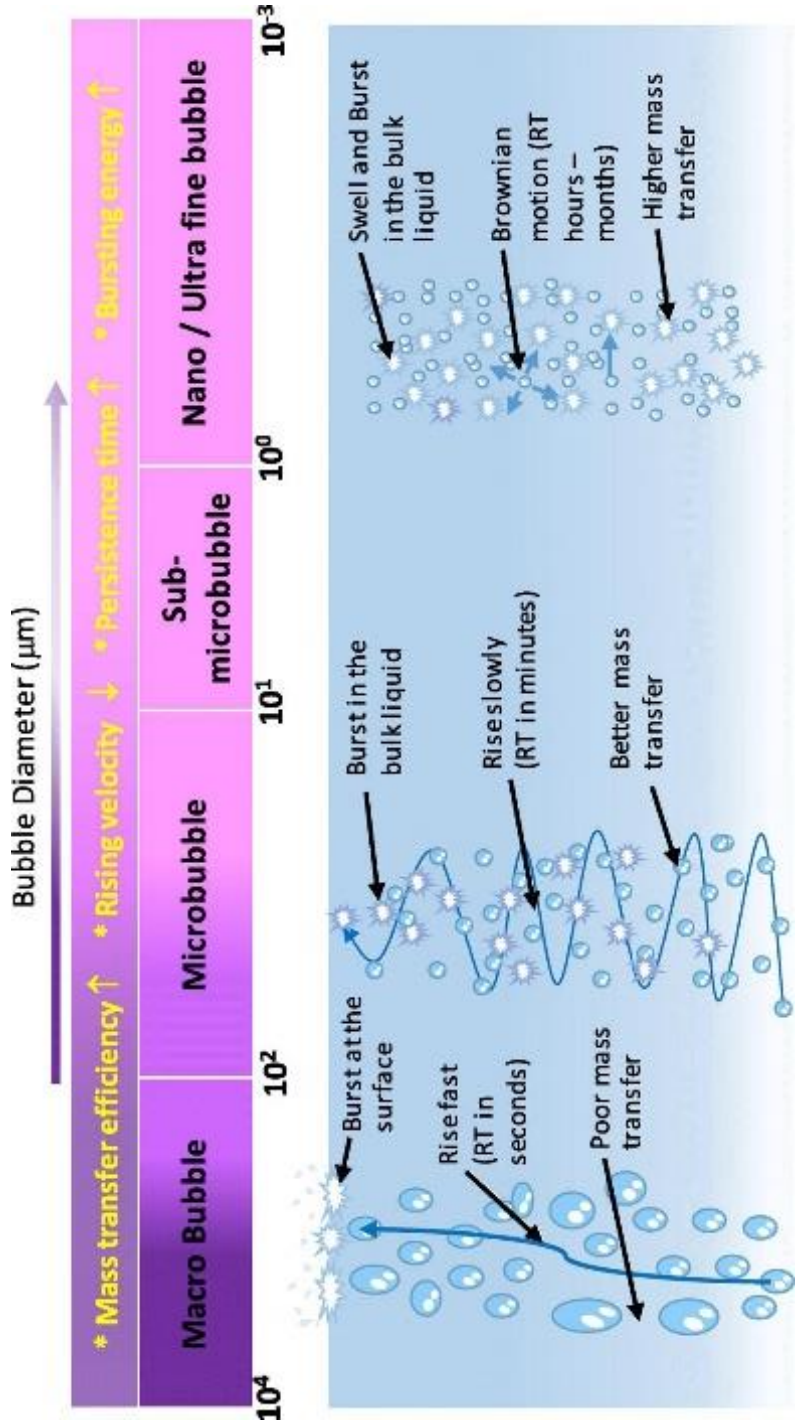

Fig. 1-1 Proposed range of the bubble sizes and major properties (Temesgen et al., 2017).

Fig. 1-2 The structure of this study.

Chapter 2 Enhanced bioconversion of hydrogen and carbon dioxide to methane using a micro-nano sparger system

2.1 Introduction

Carbon dioxide (CO_2) has been regarded as the largest contributor to the global warming, accounting for about 60% greenhouse gas effects (Francisco et al., 2010). According to a recent survey (GIO, 2015), following the energy industry, the industry and product sector (7%) is the second emission source in Japan, especially the iron and steel industry. CO_2 is usually discharged as a waste product due to its inert, non-reactive, and low Gibbs free energy properties. Various CO_2 removal technologies including absorption (Aronu et al., 2010), adsorption (Sayari et al., 2011), cryogenic distillation (Xu et al., 2014), and membranes (Zee et al., 2013) have been proposed and investigated to mitigate its emission. While, taking into consideration that CO_2 is another important carbon source, the conversion of CO_2 to chemicals and energy products that are currently produced from fossil fuels is promising due to the high potential market and promising benefits. In comparison to the chemical-based CO_2 capture, biological conversion of CO_2 together with hydrogen (H_2) to methane (CH_4) gains a particular focus, because the profits generated from CO_2 utilization can offset a portion of the capture cost under mild operational conditions (Burkhardt & Busch, 2013; Lam et al., 2012). Bioconversion of CO_2 and H_2 to CH_4 by hydrogenotrophic methanogens is of considerable interest because this process realizes energy storage and conversion, as well as biological-based CO_2 capture and sequestration technique (Jee et al., 1988a; Ju et al., 2008). The calorific value can be improved by converting nonflammable CO_2 to CH_4 (with a calorific value of 55 kJ/kg). Meanwhile, the energy donor H_2 is of special interest, as H_2 is also a co-product in the steel sector, and can be rapidly produced via water electrolysis (Hoekman et al., 2009), or obtained from biological process (bio-hydrogen) (Redwood et al., 2012; Rittmann & Herwig, 2012). CH_4 as the product of the bioconversion is also regarded as an energy carrier for electricity storage, which is more easily transported or stored than H_2 (Szuhaj et al., 2016).

However, a big obstacle to the successful development of the technology for scaling up is the poor gas-liquid mass transfer rate (k_La) of low soluble H_2 gas (Bassani et al., 2015, 2016; Diaz et al., 2015). When gas is sparged into the liquid, the k_La principally depends on the size and number of bubbles present (Jeffrey et al., 1990), which are affected by many factors such as agitation speed (Robinson and Wilke, 1973; Luo & Angelidaki, 2012), gas or liquid flow rate

(Guiot et al., 2011), reactor geometry (Jee et al., 1988; Luo and Angelidaki, 2013) and the nature of the liquid (Bredwell et al., 1997). Although there are various enhancement measures, the economic and practical viability of them should be carefully evaluated for their applications in large scale fermentation systems. Recently, a special attention has been paid to the application of micro-nano bubble (MNB) technology in many fields, including medicine science (Dixon et al., 2013), food science (Kobayashi et al., 2010), aquaculture (Kugino et al., 2016), and water remediation (Agarwal et al., 2011). Several special characteristics of MNB, such as high specific area (surface area per volume) and high stagnation in liquid phase, increase the gas dissolution. Moreover, it has been reported that the collapse of micro-bubbles, due to the high density of ions in gas-liquid interface just before the collapse, will lead to free radical generation, which might be favorable for microbial metabolism and further stimulate the bioactivity (Ushikubo et al., 2010). Up to now, however, little information can be found on the combination of MNB with methanogenesis.

In this chapter, MNBs were applied for the bioconversion of H_2 and CO_2 to CH_4, aiming at supplying a higher gas-liquid mass transfer. This was achieved by operating two bioreactors equipped with micro-nano sparger (MNS) and common micro sparger (CMS), respectively. The effect of MNBs on methanogens was evaluated by analyzing the variations of reactants and products in the two bioreactors. Also, the economical analysis was conducted to figure out the commercialization potential of MNS. In order to explore the influences of MNBs on biomethanation process, the gas-liquid mass transfer of hydrogen was also determined in this study.

2.2 Materials and methods

2.2.1 Experimental apparatus and operation conditions

This study was carried out in two identical stirred tank reactors (STRs) equipped with a micro-nano sparger (MNS) (Foamest Column 16-60, Nac sales corporation, Japan) and a common micro sparger (CMS) (HA003, Haohai, China), respectively. The two reactors have a same total volume of 1.1 L (headspace: liquid=6:5, v/v). The H_2 and CO_2 gas mixture (80/20, v/v) was transferred from the head space of the reactor to the liquid phase by a diaphragm pump (GS-6EA, E.M.P.-Japan Ltd, Japan), with a continuous recirculation rate of 40 mL/min which is the maximum rate for the MNS. A gas holder connected to the head space of the reactor was used to allow fermentation to proceed without creating vacuum and maintain a positive and constant pressure inside the reactor during the fermentation. A magnetic stirrer was employed

for both reactors to maintain mixing (500 rpm) and temperature maintenance (37 ± 2ºC). All the tube connections, stoppers, and seals were made of butyl rubber and glass. The diagram of the experimental setup in this study is illustrated in Fig. 2-1.

2.2.2 Inoculum and medium

The acclimated inocula, collected from the pond sediment (Matsumi Ike, Tsukuba campus) which has been well adapted to the H_2/CO_2 gas mixture (80/20, v/v) for 4 months' methane production, were introduced at a ratio of 1:4 (v/v) into the medium. The compositions of medium were the same as a previous study (Zhang et al.,1993).

2.2.3 Analytical methods

The contents of H_2, CO_2, and CH_4 in the gas phase were analyzed by gas chromatograph (Shimadzu GC-8A, Japan) equipped with a thermal conductivity detector connected to a chromatopac data analyzer (Shimadzu C-R4A, Japan). A stainless steel column packed with Porapak-Q was used for the analysis, with the temperatures of both detector and injector at 60ºC and of the column at 80ºC, respectively. N_2 was used as the carrier gas at an inlet pressure of 199 kPa and an outlet pressure of 150 kPa, respectively. The gas samples were taken at an interval of 24 h.

Total solid (TS), volatile solid (VS), and biomass concentration were analyzed according to the standard methods (APHA, 2005). Volatile fatty acids (VFAs) were analyzed by gas chromatography (GC–FID, Shimadzu C-R8A, Japan). The liquid samples were collected every three days, which were used for VFAs analysis after filtration through 0.22 μm filters.

The bubble size distribution from the two sparger systems was analyzed by Nano Sight (nano scale bubbles) and a high-speed camera (micro scale bubbles) with distilled water as the media. The mean bubble size was utilized for the calculation of specific surface area.

The mass transfer coefficient (k_La) of H_2 was determined before inoculation. H_2 was supplied to the reactors continuously. H_2 gas samples were collected from a three-way gas sampling port at an interval of 5 min. The first gas sample was collected at 2 min after the introduction of H_2 gas into the reactor. Once being collected, the gas sample was injected into a 20 mL sealed vial which contained some water at a same gas phase to liquid phase ratio as the reactor. Then the gas and the liquid was well mixed using a vortex mixer for 1 min and allowed 1 h to equilibrate the gas and the liquid phases. A gas sample from the head space was then taken and analyzed for gas composition in the gaseous phase using GC-TCD (Shimadzu GC-8A, Japan). The gas content in the head space was then converted to the aqueous phase

concentration according to Henry's law (Eq. (2-1)).

$$K_H = \frac{P}{X} \tag{2-1}$$

where, K_H is the Henry's law constant (atm), P is the partial pressure of gas above the aqueous phase (atm) and X is the mole fraction of gas in the solution (unitless). The Henry's law constant used for H_2 in this analysis was 7.52×10^4 atm (at 35ºC and 1 atm).

2.2.4 Calculation

(1) Determination of k_La of hydrogen

Assuming that the concentration in the liquid phase at the gas-liquid interface is in equilibrium with the gas concentration in the gaseous phase, the volumetric mass transfer coefficient (k_La) in the absence of microorganisms was determined using the following equation (Eq. (2-2)).

$$\frac{dc}{dt} = k_L a(C_i - C) \tag{2-2}$$

where, C is the gas concentration in the liquid phase (mg/L) at any given time t (min), and Ci is the saturated gas concentration (mg/L). Eq. (2-2) can be further simplified to Eq. (2-3),

$$\ln\left(\frac{C_i - C_0}{C_i - C}\right) = (k_L a)t \tag{2-3}$$

where, C_0 is the initial gas concentration in the liquid phase (mg L^{-1}).

(2) Hydrogen conversion efficiency

Hydrogen was provided as the sole electron donor for the batch experiments. As the total mass of H_2 supplied into the systems ($m_{G_{H_2,in}}$) is the sum of the mass utilized by the microbes and the mass left (effluent) in the system, the H_2 conversion efficiency (%) was calculated according to Eq. (2-4),

$$\eta_{H_2} = 100\times (m_{G_{H_2,in}} - m_{G_{H_2,eff}})/m_{G_{H_2},in} \tag{2-4}$$

where $m_{G_{H_2},in}$ is the mass flow rate of H_2 fed into the reactor per day and $m_{G_{H_2,eff}}$ is the mass flow rate of H_2 in the effluent gas. The utilized H_2 ($m_{H_2,utl}$) was the difference between $m_{G_{H_2,in}}$ and $m_{G_{H_2,eff}}$, as shown in Eq. (2-5):

$$m_{H_2,utl} = m_{G_{H_2,in}} - m_{G_{H_2,eff}} \tag{2-5}$$

$m_{H_2,utl}$ can be classified into two parts, H_2 employed for microorganisms growth (anabolism) and consumed to produce energy (catabolism). Since the H_2 as an energy source

can be transferred to VFAs as the intermediates and CH_4 as the final product, the utilized H_2 can be quantified according to Eq. (2-6).

$$m_{H_2,utl} = m_{CH_4,H_2} + m_{VFAs,H_2} + m_{growth,H_2} \quad (2\text{-}6)$$

where m_{CH_4,H_2} is the mass of CH_4 as equivalent H_2 m_{VFAs,H_2} is that of H_2 transferred into VFAs, and m_{growth,H_2} is that of H_2 employed for microbial growth.

(3) Carbon balance analysis

The carbon was supplied in three phases in this study: CO_2 (gas phase), Na_2CO_3 (liquid phase), and inoculum or biomass (solid phase), which can be expressed as follows:

$$C_{Total,in} = C_{in,G,CO_2} + C_{L,medium} + C_{S,biomass} \quad (2\text{-}7)$$

After the reaction, CO_2 can be transferred into CH_4, VFAs, and utilized for microbial growth, and other metabolites. Finally, the unreacted CO_2 was left in the system.

$$C_{Total,in} = C_{G,CH_4} + C_{G,CO_2,eff} + C_{L,VFAs} + C_{L,other} + C_{S,biomass} \quad (2\text{-}8)$$

(4) Estimation of Monod kinetic parameters for the batch experiments

In order to estimate the maximum specific growth rate (μ_{max}), the nutrients were supplied sufficiently to create the condition of nutrients concentration (C) and *Ks* (i.e. $C/(Ks + C) \approx 1$). During the exponential growth phase, the Monod equation can be simplified to Eq. (2-9).

$$\left(\frac{dX}{dt}\right)_{growth} = \mu_{max} X \quad (2\text{-}9)$$

where μ_{max} is the maximum specific growth rate (d^{-1}). Then, μ_{max} can be obtained by Eq. (2-10):

$$\mu_{max} = \frac{1}{t} ln \frac{X_t}{X_0} \quad (2\text{-}10)$$

where X_0 is the initial biomass concentration (g-biomass/L) and X_t is the biomass concentration at time *t* during exponential growth with no limitation of nutrients (g-biomass/L).

(5) Energy consumption analysis

The electricity consumed by the systems was estimated by monitoring the energy consumption of the related devices. The energy input was the sum of electricity cosumed by pumps and stirrers, as shown in Eq. (2-11):

$$E_{consumed} = E_{pump} + E_{stirrer} \quad (2\text{-}11)$$

where $E_{consumed}$, E_{pump}, and $E_{stirrer}$ are the total energy consumed by the system, the energy consumed by pump and stirrer, respectively.

The energy-product ratio (*R*) was calculated by Eq. (2-12).

$$R = \frac{Y_{CH_4,total}}{E_{consumed}} \quad (2\text{-}12)$$

where R is the energy-product ratio (L/kW), $Y_{CH_4,total}$ is the accumulated methane production during the whole experimental period (L). The energy consumption is mainly attritutable to the heat loss during the operation with a small amount utilized by the growth of microbes.

2.2.5 Statistic analysis

All the data were expressed as mean value ± standard deviation in this study. The significance of difference in the quantitative variables (e.g. CH_4 content in the output gas) between the two reactor systems was analyzed by one-way analysis of variance (ANOVA) using Origin 9.0 (Originlab, USA), and significance was assumed at $p < 0.05$. Moreover, regarding the microbial community, statistical analysis was carried out as previously described by Tsapekos et al. (2016) to identify the significant abundance difference in microorganisms among the samples.

2.3 Results and discussion

2.3.1 Bioconversion performance

(1) Methane production

To compare the effect of MNS and CMS on CH_4 production, the MNS reactor (MNSR) and CMS reactor (CMSR) systems were established to produce CH_4 from H_2 and CO_2. A start-up period was noticed in both reactors with a gradually increased methane production rate (Fig. 2-2), due to the adaption of methanogens to the new conditions. While the methane production trended to be stable from day 14 to day 45 with the maximum methane evaluation rate (MER) of 171.40 mmol/L_R/d in the MNSR. Similarly, the stable phase in the CMSR was detected from day 27 to day 50, achieving the maximum MER of 136.10 mmol/L_R/d. The delayed achievement on the maximum MER in the CMSR was most probably attributed to its lower biomass growth rate. At the very beginning, both the aqueous substrates and the gaseous substrates were sufficient for the microbes, so that the microbial growth exhibited a rapid increase which agrees with the increase in methane production, the major product in this kind of systems. However, when the biomass increased to some extent, the dissolved hydrogen concentration (DHC) became the limiting factor for the microbes, leading to the maximum methane production maintained at a stable period. From day 46 to day 51, the MER of MNSR began to decrease gradually, as a result of the exhaustion of some nutrients in the medium. The

results from this study indicate that MNSR can produce more CH_4 than CMSR.

The finding of this work is to some extent similar to that of Weimer & Zeikus (1978) who used *Methanosarcina barkeri* MS as the inoculum, achieving the MER of 5.539 mmol/L/h in a 2 L reactor under fed-batch mode conditions. Their result is comparable to the MER of CMSR, while lower than that of MNSR. The current work is also comparable to Roennow & Gunnarsson (1982) who carried out the fed-batch experiments in a 1-L reactor.

(2) H_2 utilization efficiency

In order to confirm that the enhancement on CH_4 production by MNSR was brought about by improvement of k_La using MNBs, H_2 balance analysis was used to investigate whether the bioconversion efficiency of H_2 was stimulated by the MNBs or not. The utilized H_2 concentration was calculated by Eq. (5). As shown in Fig. 2-3, H_2 was not exhausted in both MNSR and CMSR, due to the decreased dissolved H_2 concentration along with operation time, resulting in weakened driving force for gas-liquid mass transfer. As the same trend with CH_4 production, H_2 consumption increased gradually, and then became stable for some period. The maximum H_2 utilization in the MNSR was detected on day 20 with the maximum η_{H_2} of 95%. In comparison to MNSR, $m_{H_2,utl}$ in the CSR was lower, correspondingly yielding to a lower maximum η_{H_2} of 80% (day 25). This observation implies that MNS can transfer more H_2 from gas phase into liquid phase during the same operation duration compared with CMS. An ideal condition for the bioconversion is that H_2 could be transferred at a high rate without any accumulation. The maximum dissolved hydrogen concentration in the water is about 1.6 mg/L at normal pressure (Munasinghe & Khanal, 2014). While the utilized hydrogen concentration in the two reactors is much higher than 1.6 mg/L, illustrating that H_2 was consumed by the microbes. The H_2 converted to CH_4 (m_{CH_4,H_2}) was lower than the utilized H_2 concentration ($m_{H_2,utl}$), indicating that there could be a prior in biomass growth than CH_4 production. From day 20 on, the m_{CH_4,H_2} in the MNSR contributed over 95% to the total utilization of H_2, and maintained at this high proportion for about 20 days. The CH_4 production in both reactors did not show a continuous increase, demonstrating the lack of dissolved hydrogen for methanogens. Specifically, the contribution of m_{CH_4,H_2} in the CMSR to $m_{H_2,utl}$ was slightly lower (about 90%), indicating H_2 was also engaged in VFAs production and biomass growth.

2.3.2 Biomass enrichment

To determine the effect of MNBs on biomass growth, biomass concentration was

quantified in time course (Fig. 2-4). The superiority of the MNSR was not obvious till day 5. After day 5 the MNSR experienced a rapid increase in biomass and earned a higher maximum specific growth rate of 0.15 d^{-1} in comparison to 0.09 d^{-1} in the CMSR. Moreover, the total amount of biomass was much greater in MNSR than that in CMSR. Seen from the SEM images, the MNSR seems to enrich methanogens cell density more efficiently than the CMSR. These results suggest that methanogens use more dissolved H_2 in MNSR due to its higher k_La. However, the biomass concentration showed a stable trend following the rapid growth period, demonstrating that the dissolved H_2 concentration was still the limiting factor which dominates H_2 utilization for catabolism reactions (CH_4 production). The inocula used in this study was the acclimated anaerobic sludge, a mixed culture. Compared to the pure culture, generally the mixed culture is more advantageous regarding availability and cost, if not thinking about the relatively lower conversion rate due to the competitive communities. Moreover, the MNSR can be applied in large-scale tests according to the results from the acclimated anaerobic sludge.

2.3.3 Variation in volatile fatty acids (VFAs)

Anaerobic conversion of CO_2 can support a variety of microorganisms from different trophic groups within a microbial community. Therefore, the pathways involved in CH_4 production from CO_2 become more complex when taking the mixed anaerobic consortium into consideration. For a mixed methanogenic culture, i.e. the acclimated anaerobic sludge used in this study, it is essential to consider all possible reactions that are involved in the conversion of CO_2 to CH_4. The possible pathways indicate that hydrogenotrophic methanogens can directly convert H_2 and CO_2 to CH_4 through the pathway (a). On the other hand, homoacetogenic bacteria can participate in the conversion of the H_2 and CO_2 to acetate, a thermodynamically favorable reaction (pathway (b)). Then the acetoclastic methanogenesis will occur according to the pathway (c). Conversely, syntrophic acetate-oxidizing (SAO) bacteria can convert acetate to H_2 and CO_2 (pathway (d)) when acetoclastic methanogenesis is deficient (Karakashev et al., 2006). The SAO reaction becomes thermodynamically favorable at low H_2 partial pressure (< 10^{-4} atm at 35ºC) (Lee & Zinder, 1988; Cord-Ruwisch et al., 1998).

VFAs accumulation was not detectable in the MNSR during the first week (Fig. 2-5). Then VFAs concentration increased with the increase in CH_4 production. However, at the end of the experiments VFAs was not detectable in the MNSR, indicating that VFAs in this reactor experienced a production followed by consumption progress. It has been pointed out that a high dissolved H_2 concentration inhibits propionate and butyrate conversion to acetate or H_2 and

CO_2 during anaerobic digestion, yielding lower conversion rate or the whole process breakdown (Diaz et al., 2015). Thus, a higher acetic acid concentration in the MNSR can be used for more CH_4 production when compared to the CMSR, possibly contributed by the higher dissolved H_2 concentration in the reactor.

From the whole process, the concentration of total VFAs in the MNSR was lower than that in the CMSR, indicating more substrates were converted into CH_4. While, on 40th day, the higher concentration of VFAs in the MNSR was observed than the CMSR, which may be caused by the different sampling time compared with others. The H_2/CO_2 mixture gas was supplied to the reactor in one day's interval. The concentration of VFAs was varied dynamically. It may experience increase then decrease trend even in one day. The different conditions caused different reaction rates in the two reactors. Meanwhile, in the CMSR, VFAs accumulation was detected at the beginning of experiment. From day 12, the total VFAs concentration decreased while maintained at a relatively stable level, reflecting that VFAs consumption in the CMSR was not so efficient.

2.3.4 Carbon mass balance analysis

To evaluate carbon conversion efficiency in the reactors, carbon elements in the liquid, solid and gaseous phases were quantified as illustrated in Fig. 2-6. The C content in biomass was estimated according to a theoretical formula ($C_{60}H_{87}N_{12}O_{23}P$) for microbes. In addition, the calculation of $C_{L,\ TVFAs}$ was based on the individual VFA. During the wholel experiments, except for the initial carbon in the biomass and medium, the carbon input is only from CO_2 in the gas phase. The carbon balance was analyzed according to Eq. (2-8). Being consistent with the results from above two sections, a relatively more carbon conversion into the solid phase ($C_{S,\ Biomass}$) was achieved in the MNSR in comparison to the CMSR. And the final biomass yield in the MNSR was 2.34 g-biomass/L, which was 1.98 g-biomass/L in the CMSR. Anyhow, the liquid phase carbon percentage gradually was found to decrease to a low level in both reactors, which might be utilized as a source for biomass growth. Considering the gaseous phase carbon fractions, $C_{G,\ CH4}$ in the two reactors showed a remarkable difference. Still, a considerable part of CO_2 ($C_{G,\ CO2,\ Rest}$) was remained in both systems. Seen from the whole conversion process, the input CO_2 tended to be employed for microbial growth first, and then the $C_{G,CH4}$ increased with the increase in biomass growth.

2.3.5 Energy consumption

The economic and practical feasibility of this enhancement approach should be evaluated

for its applications in large scale fermentation systems. MNS clearly has a significant stimulation potential for hydrogenotrophic methanogenesis. Enrichment of methanogens in the MNSR provides a greater H_2-bioconversion potential than in the CMSR, suggesting that the gas-liquid mass transfer limitation is minimized. However, the advantage could be mitigated by high energy consumption. In this context, energy consumption analysis is essential for both the MNSR and CMSR. Table 1 summarizes the results relating to the energy consumptions by the MNSR and CMSR according to Eqs. (2-11) and (2-12).

As shown in Table 2-1, both the work of pump (E_{pump}) and stirrer ($E_{stirrer}$) in the MNSR were higher than those in the CMSR, leading to the higher energy consumption in the MNSR system. However, when evaluating the technology, the product value (CH_4 in this work) also should be taken into account. In this work, the energy-product ratio (R) was employed to represent the potential for practical application. As for the MNSR, although a higher CH_4 yield is corresponding to a higher energy consumption, its R value is still higher than the that for the CMSR, demonstrating its great potential for scaling-up application. In fact, continuous-type reactors dominate the industrial scale fermentation systems, and the methane yield can also be improved by increasing the gas recirculation rate. As proposed by Szuhaj et al. (2016), the energy for H_2 production could be supplied by the renewable resources such as the wind or solar energy. In this case, the application of MNSR for bioconversion of H_2 and CO_2 is more meaningful.

2.3.6 Gas-liquid mass transfer evaluation

In order to find out the reason for the enhancement effect by MNS, the H_2 gas-liquid mass transfer was evaluated based on the dissolved H_2 concentration. Gas mass transfer in the two reactors occurs in two zones. Mass transfer in the liquid phase is similar to that in the CSTR. Gas transfer in the headspace happens through a very thin liquid boundary layer between the bulk gas and the culture cells. The mass transfer in the liquid phase is characterized through quantification of the volumetric coefficient (k_La). Vega et al. (1989) have described the multiple steps when mass transfer occurs from gas to liquid phases, which involve (1) the absorption of a gaseous substrate across the gas-liquid interface, (2) the transfer of the dissolved gas to the fermentation media, and (3) diffusion through the culture media to the cell surface. And the most sparingly soluble gases utilized in the biochemical reactions trigger the major resistance in the liquid film around the gas-liquid interface (Klasson et al., 1992; Munasinghe and Khanal, 2010).

Because during the batch bioconversion experiments, the k_La value was continuously varying, the k_La in this study was evaluated before incubation by analyzing the dissolved H_2 concentration in the liquid. As shown in Fig. 2-7, the k_La value in the MNSR (12.95 h^{-1}) is almost twice that in the CMSR (6.60 h^{-1}), most probably due to the increase in specific surface area because of much smaller bubble size.

The specific surface area to liquid volume ratio was calculated by according to both the micro-scale and nano-scale bubble size distribution in the two reactors. The average bubble size in the CMSR and MNSR was determined as about 845 μm and 220 μm, respectively, corresponding to the specific area to liquid volume of 5,640 cm^2/L_R, and 48,042 cm^2/L_R. This specific area has been increased by one order of magnitude, implying more sufficient contact chance between methanogens and the gaseous substrates.

Results show the significant difference in the k_La value of MNSR and CMSR. As it is known, both reactor configurations and operation conditions can affect the k_La value. Smaller sparger pore size may have higher k_La value, which is also verified by this study (Table 2-2). The k_La value obtained from this study is much lower than that from Bassani et al. (2017), possibly resulted from the low recirculation rate applied in this study (40 mL/min). Thus, the followed-up experiments will be carried out to optimize the k_La value taking higher recirculation rate and higher temperature into consideration. In a summary, these results demonstrate that k_La is a key factor for the enhanced CH_4 production from the MNSR.

2.4 Summary

The enhanced bioconversion of H_2 and CO_2 to CH_4 was realized by using the MNS. The maximum MER of 171.4 $mmol/L_R/d$ in the MNSR is much higher than that in the CMSR (136.1 $mmol/L_R/d$). The MNSR also displayed superior biomass growth with specific growth rate of 0.15 d^{-1} than that of CMSR. The VFAs accumulation was not detectable in MNSR. Higher gas-liquid mass transfer was achieved in the MNSR than that in the CMSR. A higher energy-product ratio and economic analysis indicates that MNS has applicable potential for improvement of CO_2 and H_2 conversion into CH_4 in large-scale plants.

Table 2-1 Energy consumption for the two reactor systems

Reactor	E_{pump} (W)	$E_{stirrer}$ (W)	$E_{consumed}$ (W)	R (L/kW)
MNSR	2.80×10^4	1.59×10^4	4.39×10^4	1.80
CMSR	2.69×10^4	1.39×10^4	4.08×10^4	1.45

E_{pump} - the energy consumed by the pump;

$E_{stirrer}$ - the energy consumed by the stirrer;

$E_{consumed}$ - the sum of E_{pump} and $E_{stirrer}$.

Table 2-2 Comparison in k_La value among different biogas methanation systems

Bioreactor features	Sparger pore size	Working volume (L)	Cultivation modes	Inoculum	Temp. (°C)	k_La (h^{-1})	Reference
CSTR	0.5-1.0 mm/ 14-40 μm	0.6	Chemostat	Digested manure	55	6.6-16.05	Luo and Angelidaki, 2013
UBF	5 μm	19.3	Chemostat	Anaerobic granules	36 ± 2	0.72-20.86	Frigon and Guiot, 1995
CSTR	-	3.07-13.4	Fed-batch	Anaerobic sludge	32-35	0.06-0.16	Pauss et al., 1990
UASB	0.5 μm/2 μm	0.85	Chemostat	Hydrogenotrophic methanogens	55	240-776	Bassani et al., 2017
CSTR	0.2 μm-MNS/845 μm-CMS	0.5	Fed-batch	Anaerobic sludge	37	12.95-MNS/6.6-CMS	This study

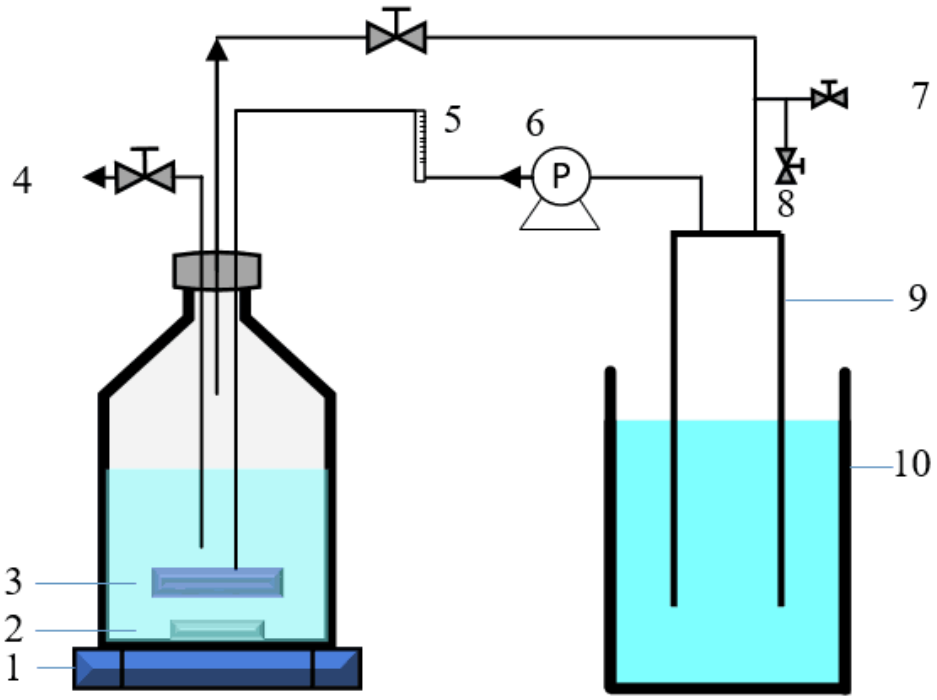

Fig. 2-1 Schematic diagram of the batch fermentation system. 1- Magnetic stirrer, 2- Rotor, 3- Micro-nano sparger (or common micro sparger), 4- Liquid sample port, 5- Flow meter, 6- Gas recirculation pump, 7- Gas input port, 8- Gas sample port, 9- Gas holder, 10- Saturated sodium bicarbonate solution.

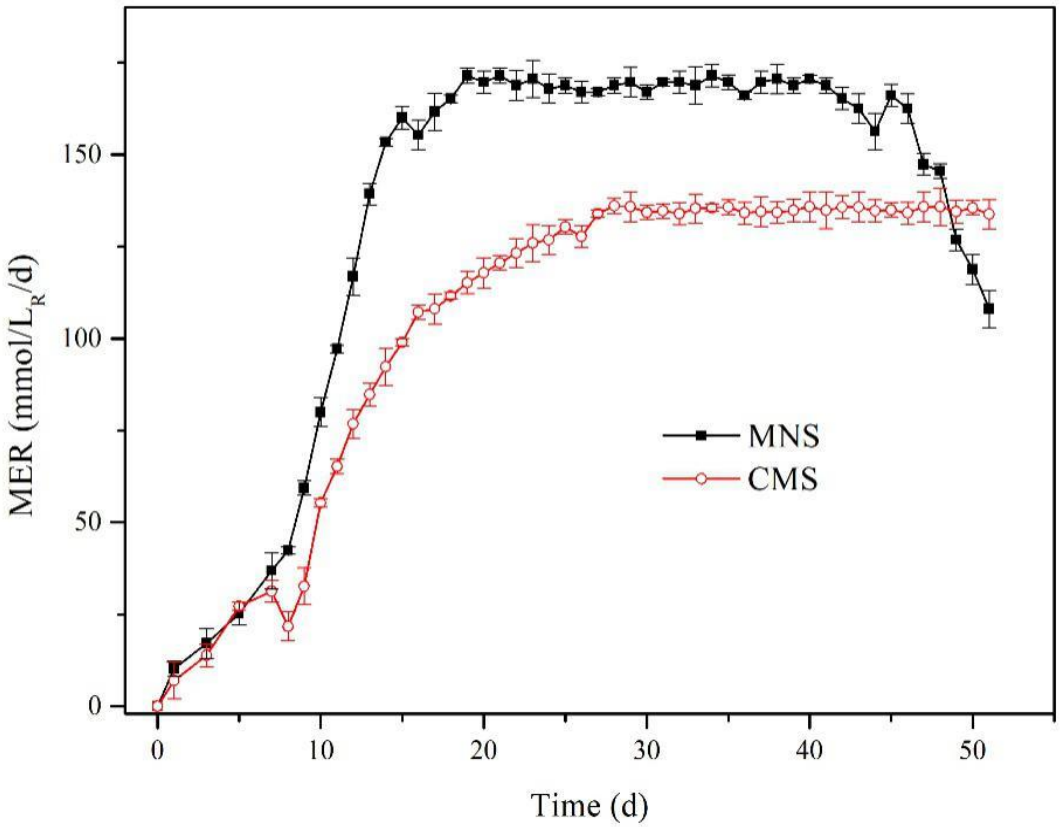

Fig. 2-2 Methane evolution rate (MER) for the two reactors. Solid squares denote MNSR (micro-nano sparger reactor) and open circles denote CMSR (common micro sparger reactor).

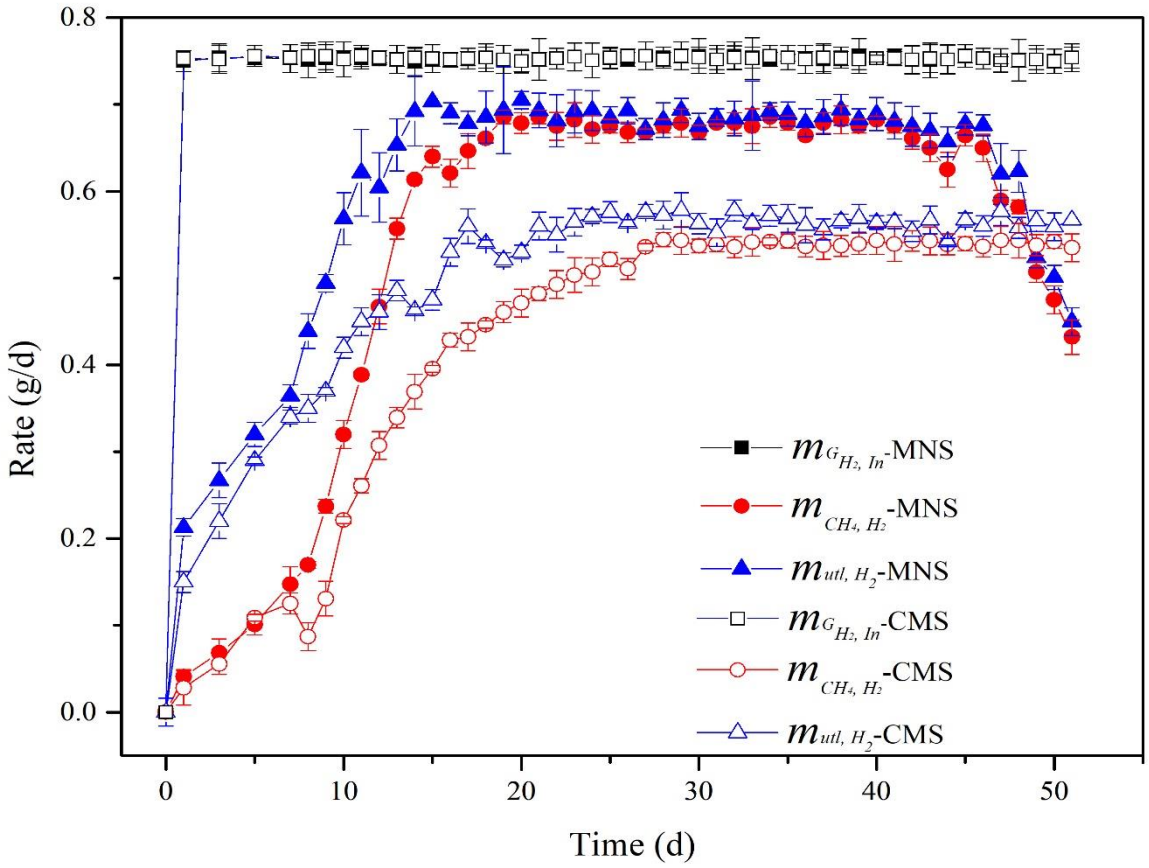

Fig. 2-3 H_2 balance analysis for the two reactor systems. Solid symbols denote the micro-nano sparger (MNS) and open symbols denote the common micro sparger (CMS) ($m_{G_{H_2,in}}$ - the mass flow rate of H_2 fed into the reactor per day; $m_{H_2,utl}$ - the utilization rate of H_2 in the reactor per day; m_{CH_4,H_2} - the yield rate of CH_4 as equivalent H_2 per day).

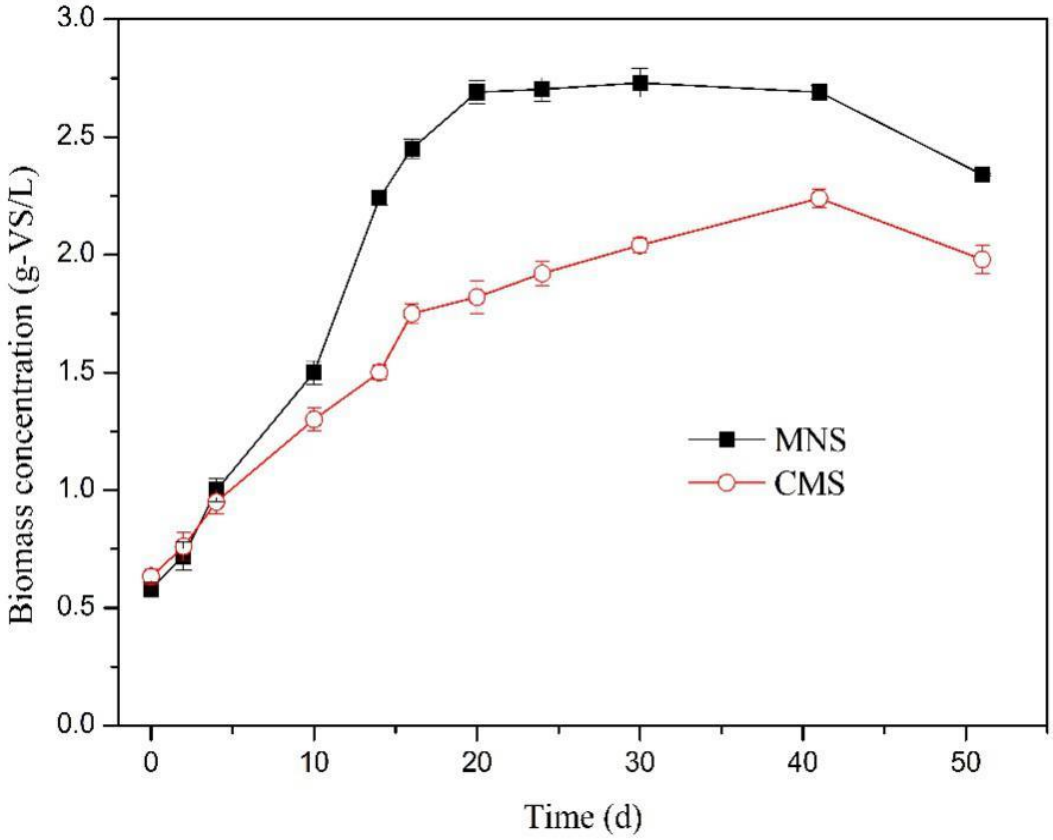

Fig. 2-4 Variation in biomass concentration in the two reactors. Solid squares denote MNSR (micro-nano sparger reactor) and open circles denote CMSR (common micro sparger reactor).

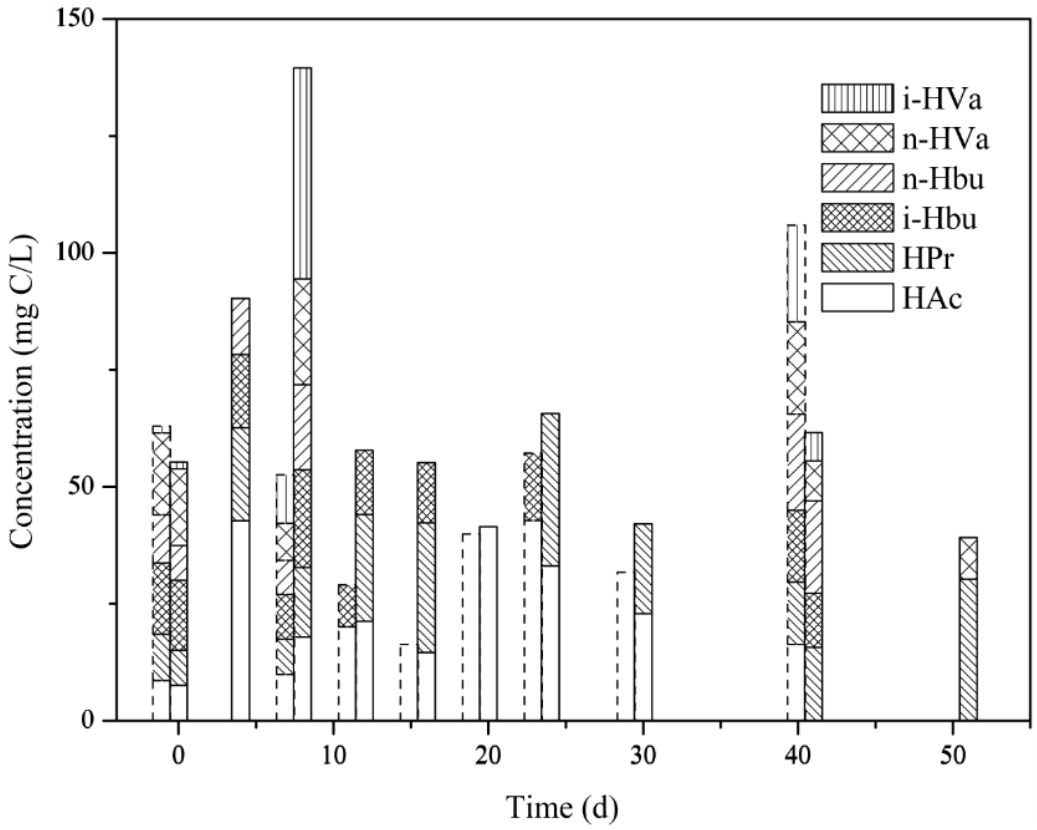

Fig. 2-5 VFAs variations in the two reactors (dashed line: MNSR - micro-nano sparger reactor; solid line: CMSR – common micro sparger reactor)

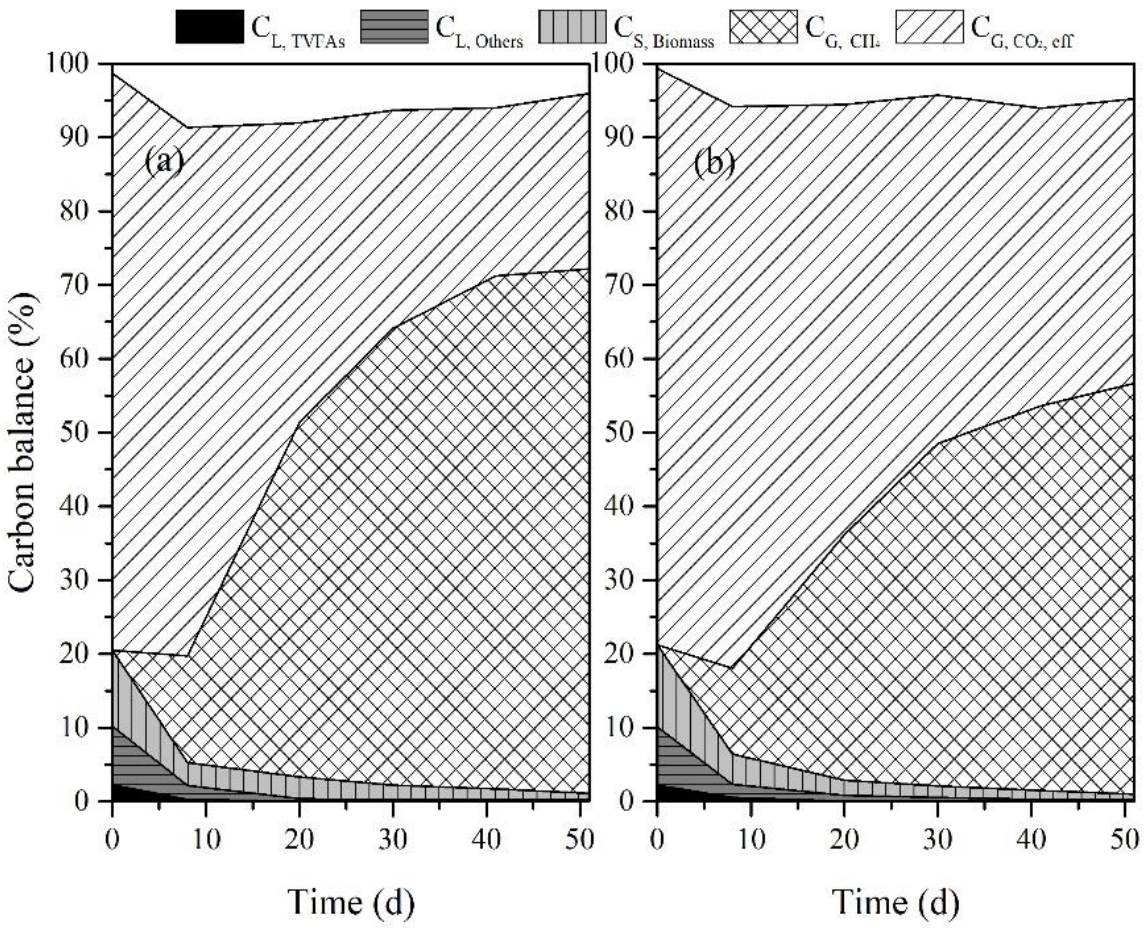

Fig. 2-6 Carbon balance analysis for MNSR (micro-nano sparger reactor) (a) and CMSR (common micro sparger reactor) (b).

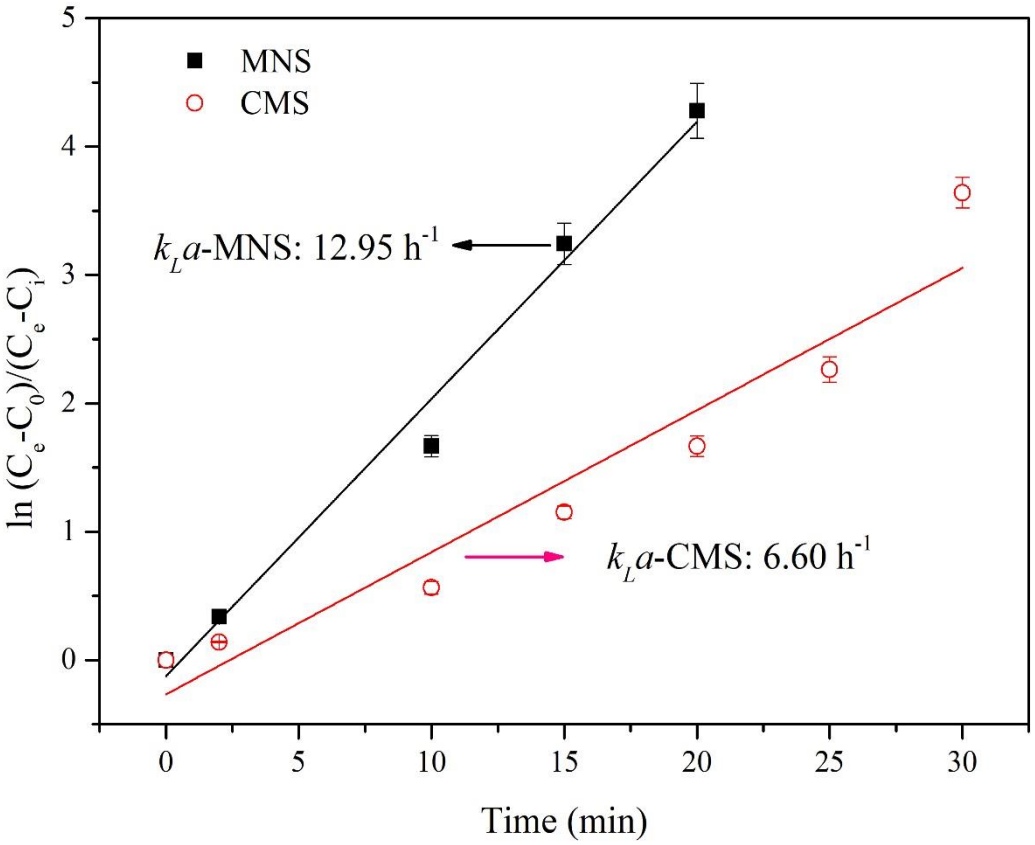

Fig. 2-7 Determination of k_La-H_2 from dissolved H_2 concentration data. Solid squares denote MNSR (micro-nano sparger reactor) and open circles denote CMSR (common micro sparger reactor).

Chapter 3 Enhanced bioconversion of H_2 and CO_2 to methane by pre-loaded bulk nano bubbles (NBs) via improving trace metal bioavailability

3.1 Introduction

As demonstrated in Chapter 2, the micro-nano bubbles, compared with the micro bubbles, significantly improved the gas-liquid mass transfer of hydrogen, while the enhancement was concluded by the enhancement of dissolution of hydrogen resulted from smaller size and correspond bigger interfacial surface area of the micro-nano bubbles. The micro bubbles may dissolve directly when introduced into the water, so that the dissolution amount was promoted obviously compared with larger bubbles. However, the bubbles in nano scale (nano bubbles, NBs) can persist in water for longer periods (Seddon et al., 2012). The stability of NBs is supported by the electrically charged liquid–gas interface, which creates repulsion forces that prevent the bubble coalescence, and by the high dissolved gas concentration in the water, which keeps a small concentration gradient between the interface and the bulk liquid (Ushikubo et al., 2010).

In this chapter, we attempted to carry out a batch experiment to verify the effect of NBs to methanogens and provide reasonable and convincing explanations of these effects.

3.2 Materials and methods

3.2.1 Medium preparation

The medium with the same components as that in Zhang et al. (1993) was prepared by distilled water and H2/CO2 NB water, respectively. For the H_2/CO_2 NB water, the components contained in the medium were first dissolved in 1 L of distilled water. Then the solution and H_2/CO_2 gas mixture (80/20, v/v) (with the flow rate of about 0.1 L/min) were introduced into a NB generator (HACK FB11, Japan) under room temperature. In order to stabilize the NB number, the medium with NBs was placed for 1 h and then stored in a sealed serum bottle.

3.2.2 Inoculation

The inocula was the same as Chapter 2 with the same inoculation ratio. The experiments were carried out in the serum bottles with the liquid and headspace volume of 50 mL and 60 mL, respectively. The H_2/CO_2 mixture gas was supplied to the headspace of the serum bottles with the pressure of 2.5 atm. The temperature was controlled at 37±2ºC. The inoculum was cultivated with the Fe-deficient medium.

3.2.3 Metal extraction and speciation

(1) Metal extraction from cells

The experimental design was shown as Table 3-1. In order to analyze the trace metal in the cell of methanogens, 10% HCl was added into the samples with twice the sample volume. Then the samples were stirred at 300 rpm for 5 min (Ginter et al., 1995). After extraction, the extracellular metals were separated from the biomass into the supernatant while the intracellular metals were remained in the biomass. The treated biomass was digested and analyzed by ICP-MS (Zhang et al., 2003).

(2) Metal speciation and mass balance analysis

The Bureau Communautaire de Reference (BCR) sequential extraction procedure modified by Sahuquillo et al. (1999), was employed to carry out metal speciation (triplicate). CH_3COOH, NH_2-OH-HCl, H_2O_2 and CH_3COONH_4 were utilized as the extraction agent to sequentially extract different fractions of metals, corresponding to soluble/exchangeable, Fe and Mn oxides, and organic matter and sulfide fractions. The content in the residual fraction was first digested according to Zhang et al. (2015), then analyzed by ICP-MS .

3.2.4 Analytical methods

The contents of H_2, CO_2, and CH_4 in the gas phase were analyzed as the same method in Chapter 2. by gas chromatograph (Shimadzu GC-8A, Japan). The gas samples were taken at an interval of 24 h.

Total solid (TS), volatile solid (VS), and biomass concentration were analyzed according to the standard methods (APHA, 2005). Volatile fatty acids (VFAs) were analyzed by gas chromatography (GC–FID, Shimadzu C-R8A, Japan).

The size distribution and number of the H_2/CO_2 NBs were measured by a nanoparticle tracking analyser (NanoSight LM-10, Malvern Instruments Ltd., Malvern, Worcestershire, UK). The zeta potential of H_2/CO_2 NBs in solution was measured by using a zeta potential analyser (Nano ZS, Malvern, UK). The pH was measured by the pH meter (B-211, Horiba, Japan). The concentration of coenzyme F_{420} was determined using a fluorescence spectrophotometer (F-4500, HITACHI, Japan) (Bashiri et al., 2010).

3.2.5 Statistical analysis

The significance of changes in methane production, VFAs variation, cell metal contents and the metal speciation (BCR extraction) between different stages of this study were assessed

by carrying out independent sample t-tests when necessary. Statistical significance was set at $p < 0.05$ (95%).

3.3 Results and discussion

3.3.1 Methane production

The daily methane yields with and without nano bubbles were summarized in Fig. 3-1. The NBW reactor showed a more excellent performance in methane production rate than the DW reactor, with the maximum daily methane production of 264.83 mL/g-VS/d and 238.05 mL/g-VS/d, respectively. Correspondingly, the average H_2 conversion efficiency improved with the presence of NBs by 4%, resulting in 66.17% of H_2 converted to CH_4 (with a maximum of 72.81%). The enhancement induced by the nanobubble group seems more obvious in the first 10 days. In the following days, the improvement showed a declining trend. These were likely due to the lifetime of nano bubbles was about 15 days (Ushikubo et al., 2010), with the decrease in bubble concentrations, the effect of nano bubbles will weaken. Albeit the H_2/CO_2 NBW reactor supplied relatively more substrates (H_2/CO_2) than the DW reactor, the amount can be eliminated considering the small bubble size and concentration. Therefore the effect of nano bubbles may be induced by other reasons. By t-test, the difference was significant with the p value lower than 0.05.

The carbon balance analysis of NBM group indicated that the introduce of H_2/CO_2 nano bubble did not cause significant increase in amount of H_2/CO_2, indicating that the enhancement for methane yield is not mainly related to the extra substrates.

3.3.2 VFA variation

The effect of nano bubbles on net VFAs yield without initial pH adjustment was shown in Fig. 3-2. It was clear that the existence of nano bubbles favored the deradation of VFAs. After 7 days' operation, a low maximum TVFAs yield of 275.47 mg/L was obtained in the NBW reactor, while higher in DW reactor (394.83 mg/L). The TVFAs trended to decrease in the following days. The VFAs detectable in this experiment were short-chain fatty acids with 2-5 carbon atoms. Acetic acid (HAc), including acetic, propionic, iso-butyric, n-butyric, iso-valeric and trace of n-valeric acids concentrations in two reactors were relatively low, indicating that the effective transformation of acetic acid to methane by aceticlastic methanogens. While the INBM group showed a higher HAc concentration but lower propionic acid (HPr) and iso-valeric acid (iso-HVa) concentration, illustrating that the conversion from HPr and iso-HVa to HAc in

the IDM reactor is relatively less efficiently than the INBM reactor. In view of VFAs variation, the NBs may also influence the transformation between the short-chain fatty acids. The conversion rate from acids with more C atoms to less C atoms was accelerated by the NBs.

As for the pH, the NBs seems no obvious effect on the pH, considering that the initial pH in the INBM reactor was 8.03, while pH of IDM reactor was 8.30, only a slight decrease, which may be cause by the existence of CO_2. The variation during the experiment was also similar, the final pH of IDM (7.56) is lower than INBM reactor (7.85) may result from the higher VFAs accumulation. pH varied in the optimal range for the growth of methanogens in the whole process (Xu et al., 2018).

3.3.3 Coenzyme F_{420} content

Coenzyme F_{420} is a unique electron carrier of Archaea and Mycobacteria. It has been shown that F_{420} is important in archaeal energy metabolism (Bashiri et al., 2010). Considering F_{420} is a unique coenzyme to methanogens, the content of coenzyme F_{420} can be indirectly attributed methanogenic activity of methanogens (Ma et al., 2013). Fig. 3-3 presents the changes of coenzyme F_{420} concentrations in the reactors. It should be noted that the relatively short experiment time of 30 d in this study may lead to no obvious variations in the microbial communities. Therefore, the methanogenic activity of the reactors can still be justified by the content of F_{420} considering the same inoculum. It was found that with the existence of NBs, the NBW reactor obtained a higher coenzyme F_{420} content. After the experiment, the concentration of F_{420} in the NBW reactor reached 1.80 μmol/g-VS, which was 1.23-fold of that in the DW reactor. The results were in consistent with the methane production enhancement and confirmed the positive effect of NBs on the coenzyme of methanogens.

3.3.4 Trace metals transformation

(1) Trace metals variation in the cells of methanogens

Previous studies showed that iron (Fe), nickel (Ni) and cobalt (Co) are essential elements for both acetoclastic and hydrogenotrophic methanogenesis. Fe and Ni formed the important subunits of enzymes such as hydrogenase and acelyl-CoA synthase involved in methanogenesis pathways (Lindahl and Chang, 2001; Thauer et al., 2010). The central site of the key enzyme in the final step of all the methanogenesis is also formed by the Ni element (Dimarco et al., 1990; Jiang et al., 2017). Cobalt is the major component of key cofactors (corrinoids) in methanogenesis pathways (Muller, 2003; Thauer et al., 2008).

The intracellular metal concentrations were obtained by addition of 10% HCl (Ginter et al.,

1995). The cells before and after HCl immersion were observed by SEM, as shown in Fig. 3-4. Before immersion, the surface of cells was rough and seemed be covered by some chemicals or crystals. After immersion by HCl, the surface of cells became smooth indicating the extracellular metals had been removed effectively.

The final VSs for INBM group and IDM group was 3.76 g/L and 3.48 g/L, respectively. Higher Fe, Ni and Co contents in the methanogens in NB group were achieved in relation to the DW group, as shown in Table 1. Among them, Fe was the most abundant for the cell pellets of the two reactors, which reached 1159.53±20.34 μg/g-VS and 1035.28±12.01 μg/g-VS in the INBM and IDM groups, respectively. While the Co content was the least abundant one, with 10.93±1.56 μg/g-VS in NBW reactor, and 7.38±1.37 μg/g-VS in DW reactor. The content of Fe was comparable with the results of Neubeck et al. (2016), while the Ni and Co concentrations in cells were higher or lower. The difference in the uptake amount of these three metals is depending on their demand by the cells and the different feeding strategy.

The deficiency of iron lead to a VFA accumulation which may be the evidence that the higher concentration of Fe uptake in the INBM group earned a lower VFA accumulation. The acidogens preferably produce butyrate and propionate to act as a feed-back metabolism to reduce the hydrogen concentration in the reactors once hydrogenotrophic methanogenesis is slower than the acetate/hydrogen production (Ketheesan and Stuckey, 2015). Moreover, the higher coenzyme content in the NBW reactor may be resulted from the more metals uptake.

(2) Trace metal speciation and mass balance analysis

In anaerobic digestion, metal nutrients are always dosed excessively in the feed to maintain the stability of the process. Whereas, the function of metal nutrients is not related to the amount of metal nutrients but correlated with their bioavailability. Because the behavior of metal nutrients may be affected by several physical indexes including pH, ORP, temperature, and chemical factors such as precipitation, adsorption, and complexation (Ketheesan et al., 2016).

Fig. 3-5 showed the mass balance of trace metals in the two reactors. The speciation of Fe, Ni and Co were analyzed by BCR extraction method. In general, the soluble and acid soluble fraction of metals are considered as the most bioavailable, which can be directly uptake by microorganisms (Gustavsson et al., 2013). The Fe-Mn oxides, and organic matter and sulfide fractions are potential bioavailable. The residual fraction is the least bioavailable fractions of metals, which is fixed in the crystal lattice of the mineral components (Ortner et al., 2015). For Fe fractions, due to the deficiency of Fe in the cultivation period, the Fe content in the seed

sludge was relatively lower than the common sludge, only 532.17 μg/g-VS. The Fe tended to transform from high bioavailability fractions (soluble and acid soluble fractions) into fractions with low bioavailability (organic matter and sulfide and residual). Compared with the IDM group, the soluble fraction in the INBM group was lower, while the acid soluble fraction was higher, leading to the high bioavailability fractions (the sum of these two fractions) were higher than that in the IDM group. Correspondingly, the lower organic matter and sulfide and residual fractions was obtained in the INBM group. Worth to mention that the organic matter and sulfide fraction in the NBW reactor was lower than the DW reactor, while the final VS in the INBM was higher than IDM group, illustrating that the Fe sulfide may decrease to some extent. This agrees with the phenomenon that after 15 days' operation, some blank particles appeared at the bottom of the DW reactor, while the NBW reactor showed a much less formation of such blank particles, which may be the metal sulfides. It has been shown that sulfide formation/dissolution showed major influence on the bioavailability of trace metals in anaerobic digestion (Gonzalez-Gil et al., 1999; van der Veen et al., 2007). Based on these results, the existence of NBs may improve the bioavailability of trace metals for the methanogens.

As for the Ni and Co fractions, there was some difference with the Fe fractions. While the trend that increase in high available fractions and decrease in low bioavailable fractions was similar.

3.3.5 Bubble size distribution and zeta potential

The distilled water with H_2/CO_2 NBs was set as the control reactor under the same condition. The concentration of NBs decreased significantly from the first day to the tenth day, from 2.35×10^7 to 6.43×10^5/mL. The size also decreased which is in consistent with the study that smaller bubbles tend to decrease the size and dissolve in the water. Zeta potential describes the charge characteristics of NBs and affects their dispersion (Li et al., 2013). High absolute value of zeta potential prevents NBs from coalescence and improves their stability. The zeta potential for NB control reactor is -43.4 mV confirming the negative charge of NBs. Although the condition for the control group is not exactly same with the other groups considering the medium and the microbes, the results showed us the lifetime for the NBs.

The bubble size distribution for NBW and medium with or without NBs were shown as Fig. 3-6. According to the results, after introduction of NBs resulted in the increased particle size in the medium, while decreased total number. Combining with the corresponding zeta potentials (Table 3-3), the supplementation of NBs decreased the zeta potential of medium, which

indicated that NBs may coagulated with the chemical particles in the medium.

It is difficult to distinguish the bubbles and the microbes or chemicals, so that the size and distribution was only done in the groups without inoculation. Suitable technologies are necessary for further analysis of mixed systems composted of nano bubble and microbes.

3.3.6 Possible mechanism for the enhancement

The trace metal bioavailability depends on not only biological (transport across membrane), but also physical-chemical processes (diffusion and dissociation of metal complexes) (Worms et al., 2006). Specially, the physical-chemical processes will change the existing state of trace metals. However, there is a paucity of quantitative data to reveal which stage is the limitation step of metal bio-uptake, including diffusion, chemical dissociation, adsorption to the microbial interface, or transfer through the plasma membrane (Wilkinson and Buffle, 2004). Several factors including the characteristics of precipitate, the degree of coprecipitation and adsorption and the size of particles play an important role.

It is a complex process for the gas fermentation. Taking the three kinds of species in the system in account, the bubbles, particles, and microbes may interact each other. Wu et al. (2015) demonstrated that the dispersion, electrostatic double layer, and hydrophobic forces governed the interaction energy, and further determined the degree of attachment between gas bubbles and particles. We assume the mechanism for the enhancement induced by the NBs is bound up with the bubble-microorganism or bubble-particle interactions in the reactor. The NBs existed in the solution may aggregate with the particles in the reactor by collision derived by shaking, just like the flotation procedure. Recently, Zhang et al. (2016) proposed that for nano scale particles, the NBs may interact with them by new nucleation on the nano particles. The NBs may also adsorb the positive ions in the medium by electrostatic attraction in view of the negative charge characteristics.

Mishchuk et al. (2006) put forward that NBs coated on the surface of particles had a profound effect on the correlation between particles and bubbles, and, specially, significantly decreases the critical particle size for coagulation. Xie et al. (2018) studied the interaction between air NBs and bitumen surfaces in the aqueous media. Results showed that the attachment of bubble-bitumen was inhibited by the electrical double layer (EDL) repulsion under low concentration of NaCl. While in 500 mM NaCl, the bubble-bitumen attachment could be induced by the hydrophobic attraction. Consequently, the high ion concentrations in the medium is favor to the bubble-particle attachment.

Fig. 3-7 showed the possible pathway for trace metals transferred into the cells. Taking Fe as an example, Fe was added into the reactor as ion form, then it experienced the diffusion procedure to shorten the distance with the microbe cells. Then certain amount of ionic Fe is transferred into different types of complexes. What's more, Fe will also react with the sulfide which is the product by the anaerobic reduction of cysteine, to form the Fe sulfide. NBs may serve as a media between the ionic Fe and the surface of the cells. What's more, even the undissolved Fe species could also coagulate with NBs due to the long-term hydrophobic attraction force. Considering the hydrophobic characteristics of the membrane of cells, the NBs may also tend to attach on the cell surface. The NBs on the surface of the particles and the cells will accelerate the aggregation of particles and cells. Based on these, the existence of NBs may "bring" more different type of Fe to the surface of the cells, so that supplied more chance for the uptake of Fe by the cells, further enhance the efficiency of Fe transfer from the extracellular to the intercellular. Cause more Fe was combined with other complexes, the formation of Fe sulfide was decreased which can explain the less darker color in the INBM group than IDM group.

The possible pathways for the effect of NBs were proposed according to the phenomenon and results in this study, while it have not been verified. It is a pity for this study did not test the forces between the particles and bubbles using some technology such as the atomic force microscopy to reveal the interactions between bubbles and microbes directly. This section will be taken into consideration in the future study.

3.4 Summary

Effect of nano bubbles (NBs) on the hydrogenotrophic methanogens was investigated by preparing liquid medium with or without H_2/CO_2 mixture nano bubbles. Results showed that enhanced methane production with pre-supplied NBs was achieved with a maximum daily methane yield of 264. 53 mL/g-VS, while 238.05 mL/g-VS without NBs. The higher coenzyme F_{420} content was obtained in the group with NBs, which is 1.23 fold than control group. 12% increment of intracellular iron content was realized with the existence of NBs, which can be the evidence for the higher coenzyme content. For the trace metal speciation, the higher percentage of acid soluble and exchangeable fraction, while lower percentage of organic matter and sulfide fractions in the group with NBs were achieved than the control group. The nano bubbles may enhance the mass transfer and metal bioavailability of trace metals. This study indicates that the bulk nano bubbles have the potential for the enhancement of methane production or other

microbial stimulation.

Table 3-1 Summary of experimental design

Groups	Conditions			Indexes	Objectives
	Methanogens	H_2/CO_2 nano bubbles	Medium components		
INBM	+	+	+	Gaseous: H_2, CO_2 & CH_4 Liquid: VFAs & TOC Solid: TS & VS	Investigate the effect of nano bubbles on methanogenesis
IDM	+	−	+	Coenzyme content Intracellular metal concentration Metal speciation	Explore the mechanism of the effect (the microbial activity & trace metal mass transfer)
NBM	−	+	+	Gaseous: H_2, CO_2	Evaluate the effect of nano bubbles for the physicochemical properties of medium and water
DM	−	−	+	Liquid: TOC Metal concentration Bubble size distribution Zeta potential	
NBW	−	+	−		
DW	−	−	−		

*INBM - Isolated medium with H_2/CO_2 nano bubbles;

IDM – Isolated medium without nano bubbles;

NBM – Pure medium with nano bubbles;

DM – Pure medium without nano bubbles;

NBW – Distilled water with nano bubbles;

DW – Distilled water without nano bubbles.

Table 3-2 Trace metals in cells for IDM and INBM groups

	Trace metals in cells (μg/g-VS)		
	Fe	Ni	Co
IDM	1035.28±12.01	59.14±3.29	7.38±1.37
INBM	1159.53±20.34	63.13±2.72	10.93±1.56

*IDM - Isolated medium without nano bubbles;

INBM - Isolated medium with nano bubbles

Table 3-3 Bubble size and number and zeta potential for groups without inoculum.

Groups	Mean particle size (nm)	Total particle number (/mL)	Zeta potential (mV)
NBW-10	158.8±58.6	$1.94\times10^{7}\pm1.42\times10^{7}$	-19.5± 0.8
DM-10	187.5±6.9	$7.12\times10^{8}\pm3.42\times10^{7}$	-31.8±0.9
NBM-10	220.4±3.9	$6.98\times10^{8}\pm2.17\times10^{7}$	-28.8±3.0

⁎NBW-10 – the distilled water with nano bubbles on the 10^{th} day;

DM-10 – the pure medium without nano bubbles on the 10^{th} day;

NBM-10 – the pure medium with nano bubbles on the 10^{th} day.

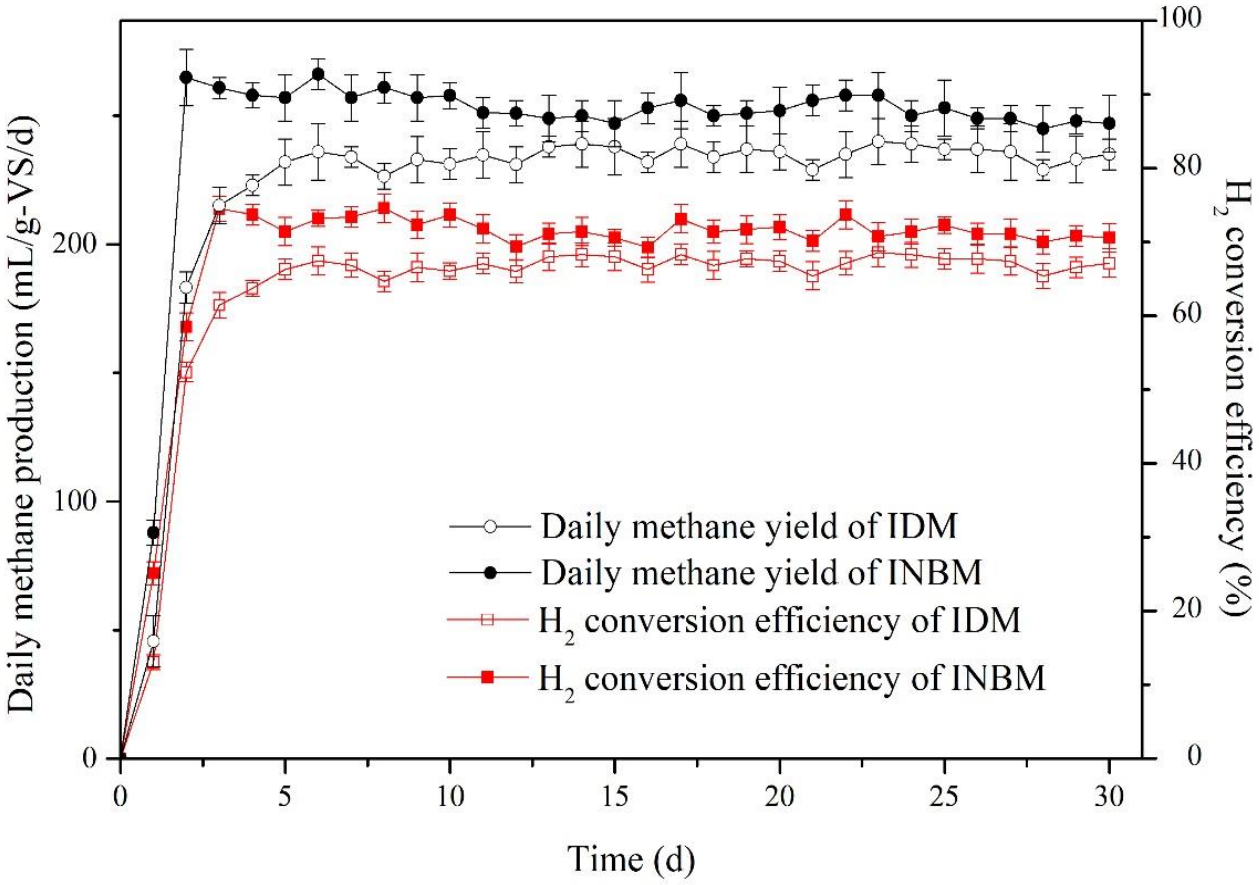

Fig. 3-1 Methane production and H_2 conversion efficiency of IDM (isolated medium without nano bubbles) and INBM (isolated medium with nano bubbles) groups.

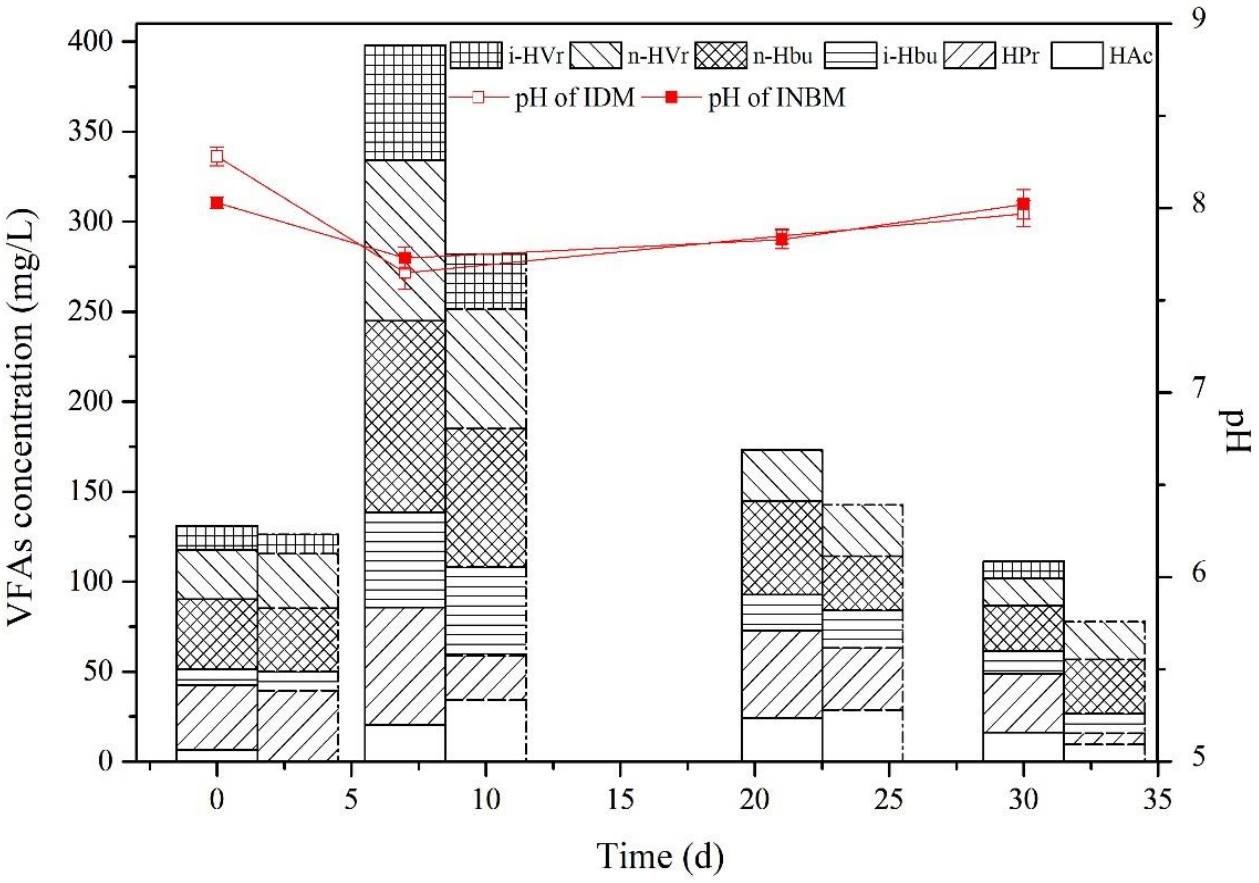

Fig. 3-2 VFAs and pH variation in the IDM (isolated medium without nano bubbles and INBM (isolated medium with nano bubbles) groups (Solid line: IDM, dashed line: INBM).

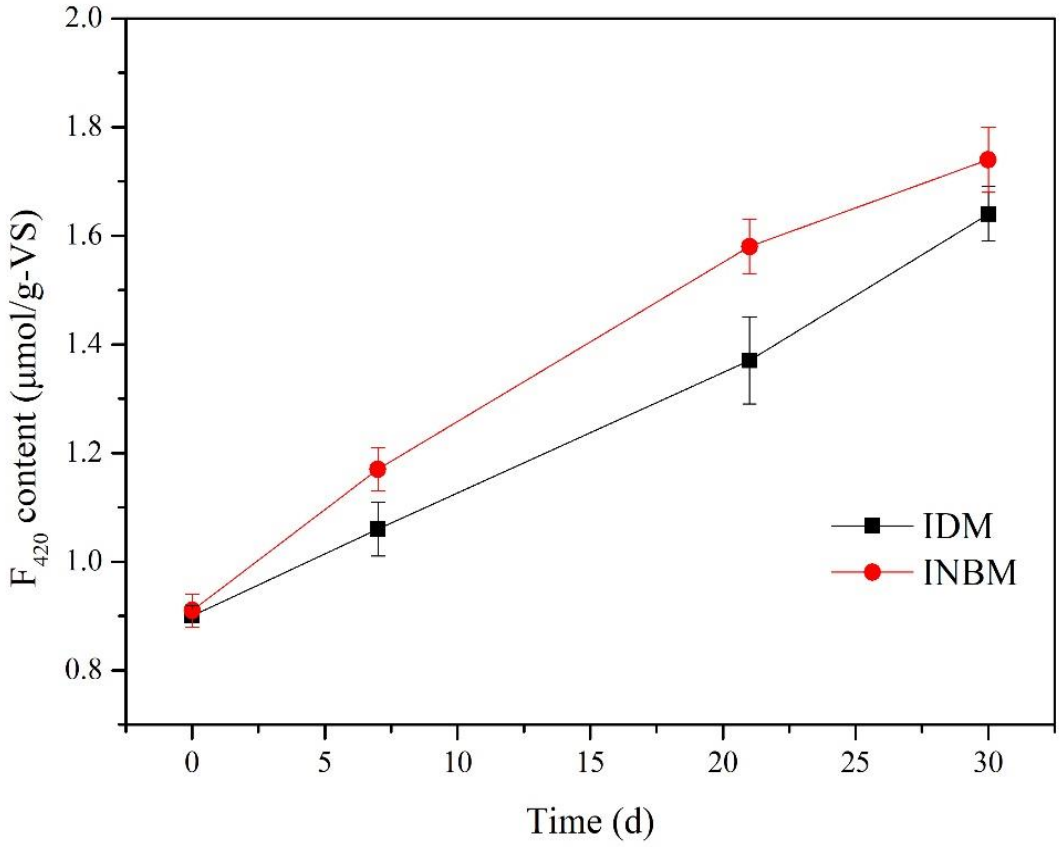

Fig. 3-3 Coenzyme F_{420} content in the IDM (isolated medium without nano bubbles) and INBM (isolated medium with nano bubbles) groups during the gas fermentation.

(a)

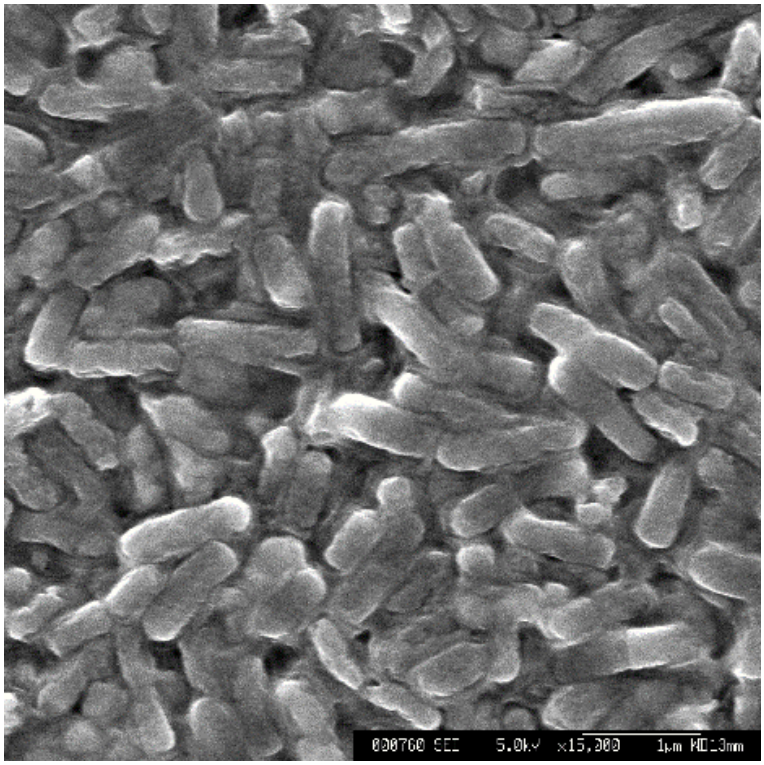

(b)

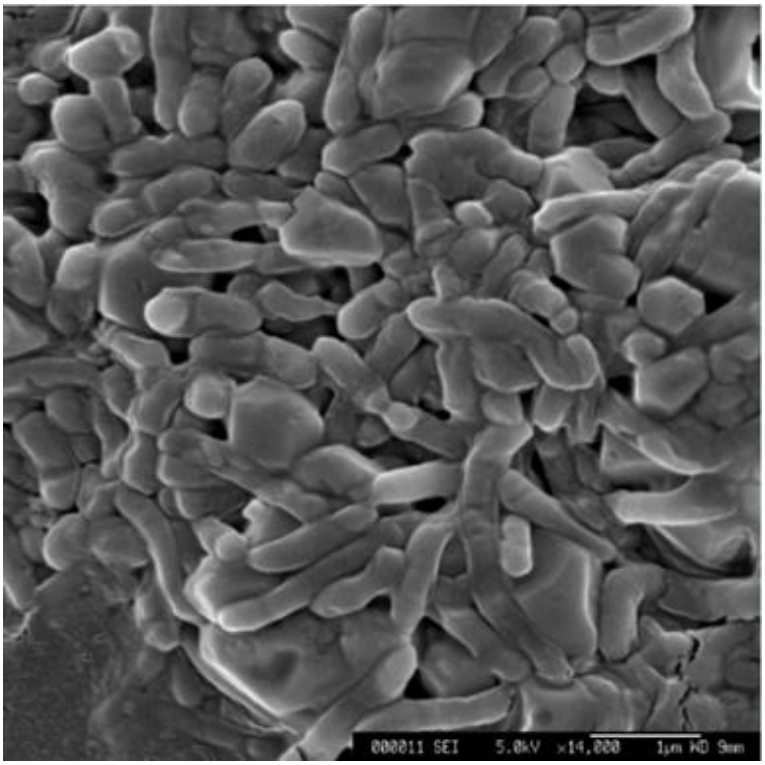

Fig. 3-4 SEM images for the methanogen cells before (a) and after (b) extraction with 10% HCl.

(a)

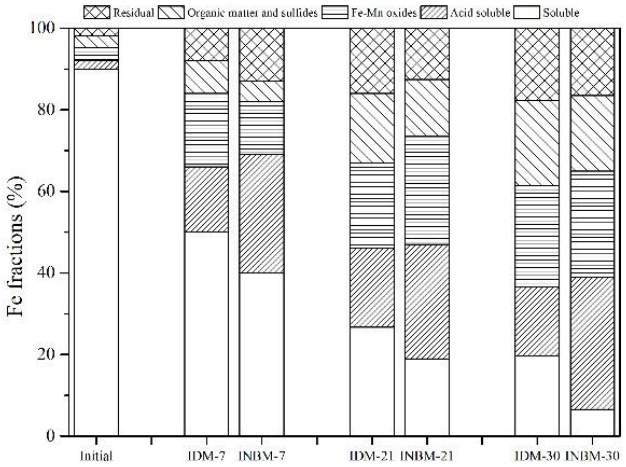

(b)

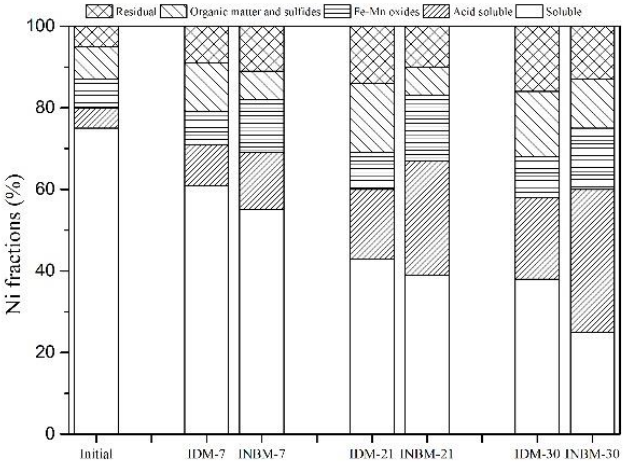

(c)

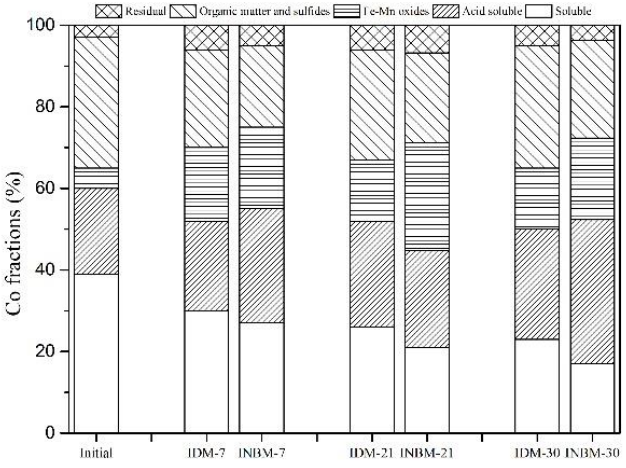

Fig. 3-5 Metals speciation for the IDM (isolated medium without nano bubbles) and INBM (isolated medium with nano bubbles) groups (a) Fe fractions; (b) Ni fractions; (c) Co fractions.

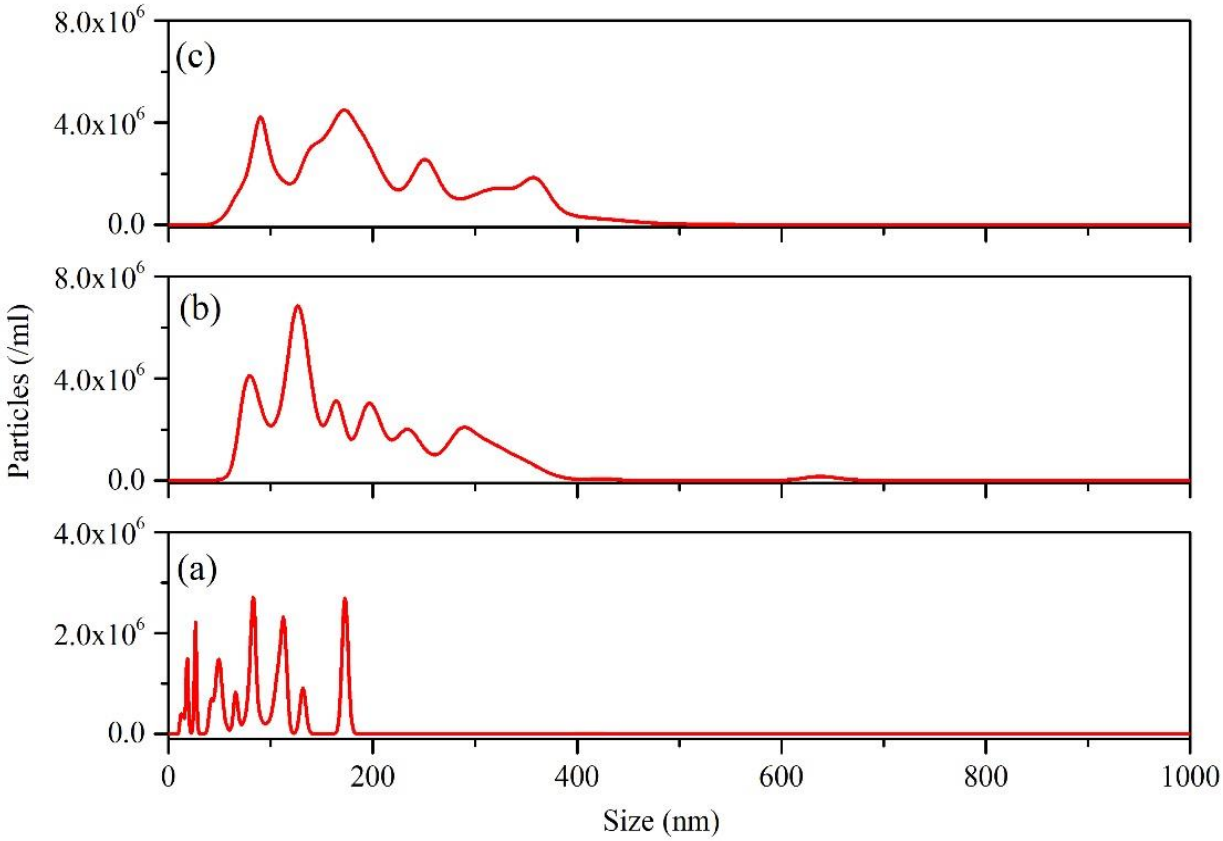

Fig. 3-6 Particles distribution for different groups (a) NBW (distilled water with nano bubbles); (b) DM (pure medium without nano bubbles) (c) NBM (pure medium with nano bubbles).

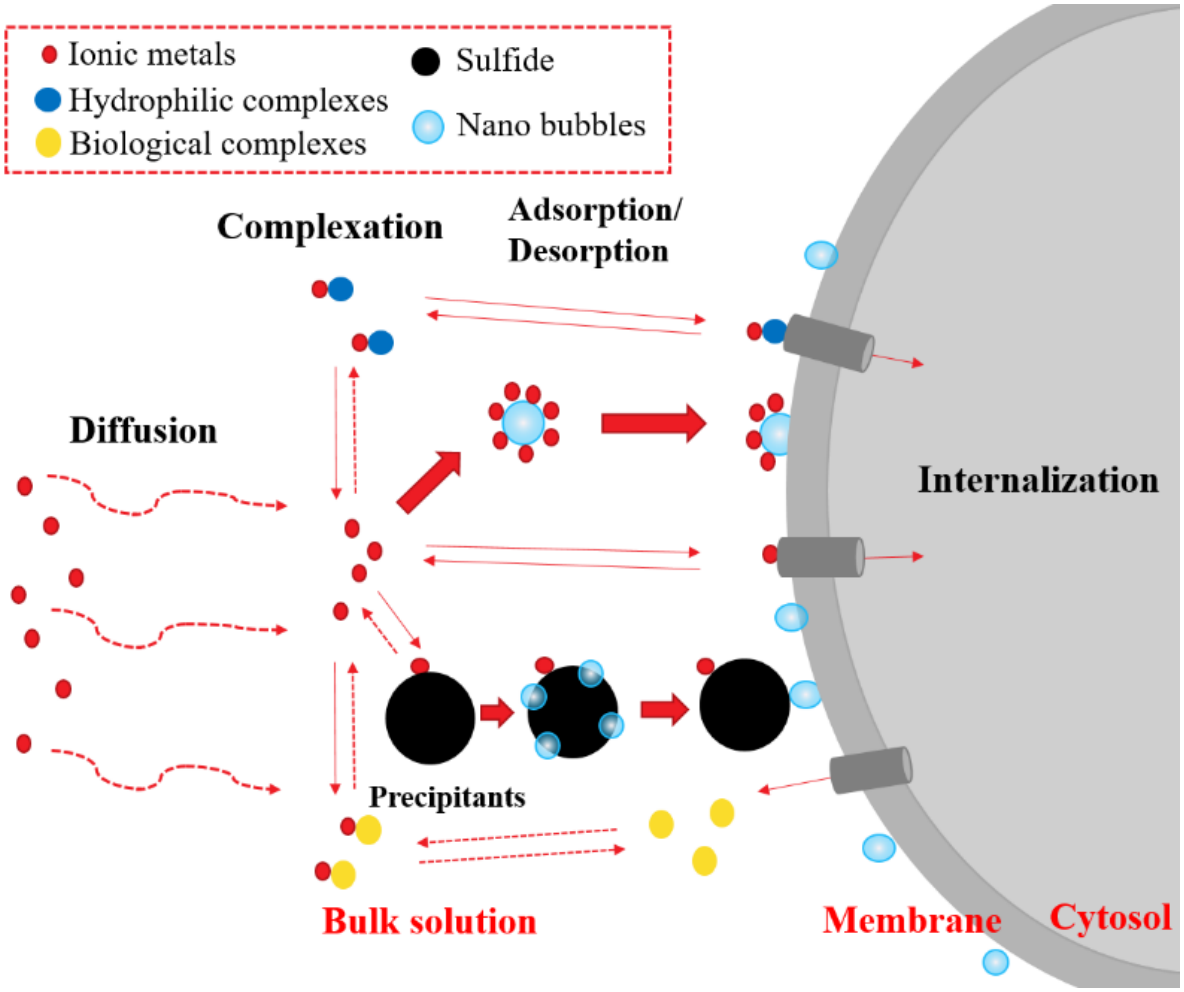

Fig. 3-7 Conceptual model of some of the important physicochemical processes leading to and following the uptake of a trace metal by a methanogen with the existence of NBs. Pathways with solid or dashed narrow arrow stand for the common processes. Pathways with wide arrow stand for the special processes with the existence of NBs.

Chapter 4 The effect of air nano bubbles on iron bioavailability in anaerobic digester under varied iron and sulfur concentrations

4.1 Introduction

Oxygen has often been considered an inhibitor of methanogenesis (Chu et al., 2005). Aeration may result in the oxidation of part of the substrate and the inhibition of anaerobic archaea activity. However, provided the amount is controlled in a suitable range, it may alleviate the acidification due to accumulation of VFAs and consequent decrease in pH, subsequently enhance the methane production (Botheju et al., 2010). On the other hand, aerobic treatment may also enhance hydrolysis procedure by stimulating the activity of hydrolysing bacteria (Hao et al., 2009). Moreover, micro-aeration may be of use in reducing sulphides content and, therefore, minimizing the toxic effect of aqueous sulphides on acetogenic, methanogenic microorganisms (Krayzelova et al., 2015; Nghiem et al., 2014). Whereas, the effect of micro-aeration on the bioavailability of trace metals and further the methanogenesis has yet been explored in depth.

The air micro-nano bubbles exhibited beneficial to the germination of plant seed and the growth of mice and fish, due to the generation of ROS during the collapse of bubbles (Liu et al., 2016). The pre-loaded air nano bubbles may also influence the methanation and microbe growth, while it is worthy to explore whether the effect was caused by the micro-aeration (dissolved oxygen) or the existence of nano bubbles.

During anaerobic digestion, iron is an essential component of some cofactors and enzymes that stimulate the biogas process performance, with the largest content in the methanogens cells among the trace metals (Scherer et al., 1981). The effect of metals is not dependent on the total metal concentration, but the bioavailability of metals, because the chemical forms of the metals, and the different physical parameters (pH and redox potential) can also affect the solubility of metals (Ketheesan et al., 2016). Accordingly, the high bioavailability of Fe is beneficial to the methanogenesis process.

In this chapter, we introduced the air nano bubbles into the anaerobic digester. Based on the conclusion of last section, we focused on the trace metal (Fe) bioavailability under varied Fe and sulfur concentrations. The objective of this chapter is to investigate the effect of air nano-bubbles on bioconversion of CO_2 and H_2 to CH_4 under different iron and sulphide concentrations. Moreover, to reveal the effects were caused by the micro-aeration condition (oxygen) or the interaction resulting from the NBs.

4.2 Materials and methods

4.2.1 Medium preparation

The medium same as Zhang et al. (1993) was prepared by distilled water (DW) and air nanobubble water (NBW), respectively. For the air NBW, the components contained in the medium were first dissolved in 1 L of distilled water. Then the solution and air were introduced into a NB generator (HACK FB11, Japan) at the room temperature and a standard atmosphere. Under the above conditions. The flow rate of air was about 0.1 L/min. The medium was stored in a sealed serum bottle at room temperature after 1 h of bubble generation, to guarantee the stabilization of bubble number.

4.2.2 Inoculation

The acclimated inocula, collected from the pond sediment (Matsumi Ike, Tsukuba campus) which has been well adapted to the H_2/CO_2 gas mixture (80/20, v/v) for 4 months' methane production, were introduced at a ratio of 1:9 (v/v) into the medium. The experiments was carried out in the serum bottles with the liquid and headspace volume of 50 mL and 60 mL, respectively. The H_2/CO_2 mixture gas was supplied to the headtop of the serum bottles with the pressure of 2.5 atm. The gas was supplied in fed-batch mode, while the medium was in batch mode. The temperature was controlled at 37±2ºC. During cultivation, the supplied medium was without Fe addition.

4.2.3 Metal speciation and mass balance analysis

The metal speciation was carried out according to the method of Stover et al. (1976). A description of the extraction procedure is given in Table 4-1. The total metal content in the sludge, and the residual fraction after sequential extraction was digested according to Zhang et al. (2015). Then the digested samples were analyzed by ICP-MS.

The experimental design of batch trials was summarized and shown in Table 4-2. In order to investigate the effect of air-NBs on methane production under different iron concentrations, varing concentrations of Fe (0, 50, 100 μM) were added to different batch bottles respecitively. Meanwhile, the cysteine was utilized as the sulfur source for methanogens with varied initial concentration of 0, 3, 6 mM.

4.2.4 Analytical methods

The contents of H_2, CO_2, and CH_4 in the gas phase were analyzed as the same method in

Chapter 2. The gas samples were taken at an interval of 24 h.

Total solid (TS), volatile solid (VS), and biomass concentration were analyzed according to the standard methods (APHA, 2005). Volatile fatty acids (VFAs) were analyzed by gas chromatography (GC–FID, Shimadzu C-R8A, Japan).

The size distribution and number of the air NBs were measured by a nanoparticle tracking analyser (NanoSight LM-10, Malvern Instruments Ltd., Malvern, Worcestershire, UK). The zeta potential of air NBs in solution was measured by using a zeta potential analyser (Nano ZS, Malvern, UK). The pH was measured by the pH meter (B-211, Horiba, Japan). The oxidation-reduction potential (ORP) was detected by the ORP meter (YK-23RP, Lutron, Taiwan).

4.2.5 Statistical analysis

The significance of changes in methane production, VFAs variation, intracellular metal contents and the metal speciation in different stages of this study were assessed by carrying out independent sample t-tests when necessary. Statistical significance was set at $p < 0.05$ (95%).

4.3 Results and discussion

4.3.1 The effect of nano bubbles on the medium without methanogens

The bubble size distribution for NBW and medium with or without NBs were shown as Table 4-3. According to the results, after introduction of NBs resulted in the increased particle size in the medium, while decreased total number. Combining with the corresponding zeta potentials (Table 4-3), the supplementation of NBs decreased the zeta potential of medium, which indicated that NBs may coagulated with the chemical particles in the medium. The oxidation-reduction potential (ORP) was also measured to evaluate the effect of air on the physical-chemical properties of the medium. The introduction of NBs only resulted in a slight decrease in ORP due to the creation of anaerobic environment. Therefore, the existence of nano bubbles may not affect the ORP very obviously.

The Fe speciation under different conditions in DM and NBM groups were shown as Fig. 4-1. Results showed that the existence of air NBs will improve the percentage of soluble fractions, in other words, less precipitations occurred in the NBM group. The variation of Fe concentration lead to a more significant change for the fractions than altering cysteine concentrations.

4.3.2 Effect of Fe concentrations

Trace metals are components of the essential enzymes, which can catalyse various

anaerobic biochemical reactions. Zayed and Winter (2000) analysed the metal content in the cell of ten methanogenic strains, and results showed that Fe content was the highest in the methanogenic strain cells, compared with Zn, Ni, Co, Mo and Cu. The effect of metals is not dependent on the total metal concentration, but the bioavailability of metals, because the chemical forms of the metals, and the different physical parameters (pH and redox potential) can also affect the solubility of metals. The excess concentration of metals may damage the disruption of enzyme function and structure due to binding of metals with functional groups on protein or the substitution of essential metals in enzymes (Chen et al. 2008a, b). It is generally believed that acidogens are more resistant to heavy metal toxicity than methanogens (Mudhoo et al., 2013).

(1) Methane production

In order to investigate the effect of air-NBs on methane production under different iron concentrations, varing concentrations of Fe were added to the batch bottles. Fig. 4-2 showed the methane production for different groups under varied Fe concentrations.

It was found that the supplementation of Fe showed the stimulation of methane yields under low and moderate concentrations. However, after reaching maximum methane yield at 50 μM (395.14 mL/g-VS for IDM group, 428.17 mL/g-VS for INBM, respectively), the further increased concentrations of Fe (100 μM) led to the decreased methane yield. The excessive supplementation of Fe exhibited the obvious inhibition to methanogens. The results of Su et al. (2015) showed that the high concentration of Fe lead to the decreased availability of P, which may due in part to the decreased bioavailability of nutrients.

The air-NBs showed positive effect on the methane yield with the Fe concentration of 0, 50 μM. The maximum enhancement was achieved at 0 μM with an increase of 30.78%. While the increment was the lowest for groups with 50 μM Fe addition. Interestingly, supplementation of 100 μM Fe caused a stronger inhibition for INBM than IDM group (with the methane yield of 308.32 mL/g-VS and 371.90 mL/g-VS, respectively). The inhibition concentration of Fe was different with the other study (Zhang et al., 2015), which may be resulted from the different microbial composition, one of the more convincing way to evaluate the effect of Fe concentrations may be to calculate the ratio of Fe concentration and the VS, to get the specific Fe concentration.

(2) VFAs variation

Supplementation of Fe also affected the VFAs production and degradation (Fig. 4-3). For

both group, after 7 days fermentation, acetic acid was dominant in VFAs production. The total VFAs production was lowest under Fe concentration of 50 μM. Both the deficiency and excessive dose of Fe will lead to the accumulation of VFAs. The VFAs accumulation reached maximum value of 450.68 mg/L for IDM group at Fe concentration of 100 μM, indicating that the acidegens may tolerate higher Fe concentrations than methanogens.

Propionate to methane conversion involves the activity of propionate oxidizing bacteria as well as the hydrogenotrophic and acetoclastic methanogens (de Bok et al., 2004). Therefore, not only the propionate oxidizing bacteria but also the hydrogenotrophic and acetclastic methogens may contribute to the conversion of propionate to methane. As evidenced by acetate can still be directly converted into methane by acetoclastic methanogens under high Fe concentrations, acetoclastic methanogens were more constrained by Fe deficiency in comparation with the other methaogens (Ketheesan et al., 2016). Taking these into consideration, the deficiency of Fe may lead to the accumulation of acetate.

(3) Fe speciation

To examine the dynamics of Fe speciation under different Fe concentrations for both IDM and INBM groups under different Fe concentrations, the Fe fractions were extracted sequentially to determine the availability of Fe in solid matrics. To date, the trace metals contained in anaerobic sludge can be sequentially extracted by a variety of approaches (Stover et al., 1976; Tessier et al., 1979; Lake et al., 1985; Osuna et al., 2004). However, the reason for choosing the scheme proposed by Stover et al. (1976) and modified by Lake et al. (1985) in this study was that the metal sulphide fractions can be clearly differentiated.

As shown in Fig. 4-4, the Fe fractions in the inoculum were dominated by organically bounded (S3), adsorbed (S2) and sulfides (S5). Cause the inoculum was supplied without Fe addition during acclimation, the initial composition was different with the study of Ketheesan et al. (2016), which stated Fe initially accumulated in the inoculum as sulphides, carbonate/phosphates and non-defined forms (residuals) due to a prolonged supply of Fe in the seed.

After 7 days fermentation, the fraction distribution changed under different Fe supplementation. Worth to mention that, the sulfur content in the medium was increased from 1 μM (acclimation period) to 3 μM (batch fermentation), resulting in an obvious increase in the sulfides (S5) and carbonate/phosphates compared with the initial samples, while declined percentage of organically bounded fraction (from 71.53% to 30%~40%) for the groups with

different Fe supplementation. The variation indicated that the increase in sulfur supply could induce the enhanced formation of sulfides.

As for the comparison of IDM and INBM group, under 50 and 100 μM Fe concentrations, the transformation from liquid phase (soluble fraction) to solid phase (the sum of S1 to S6 fractions) was enhanced by the air NBs. The Fe bounded by electrostatic attraction (S1) and adsorbed to the methanogens (S2) for the INBM group were higher than the IDM group. While, the fraction of sulfide may decrease by the introduction of NBs. These were in consistence with the mechanism we proposed in the previous study that the existence of nano bubbles may "bring" more metal ions and sulfides to the surface of cells and improve the bioavailability and bio-uptake of metals.

(4) Soluble sulfides

Methanogenic bacteria are known to require reduced sulphur, e.g. sulfide or cysteine, as a source of a sulfur for growth (Bryant et al., 1971). So that the cysteine will experience the anaerobic degradation and be reduced to sulfides. Some part will be utilized for microbial growth, while the other part will react with metal ions or some other chemical components to form the sulfides. According to Fig. 4-5, the soluble sulfides decreased with the increase in Fe. And the highest level was reached by the groups without Fe addition (1.29 mg/L for IDM and 1.06 mg/L for INBM, respectively). Accordingly, the increase of Fe concentration will lead to the significant decrease of soluble sulfides.

Under different Fe concentrations, the soluble sulfide in IDM group is lower than INBM group. While, if the stimulation was caused by the oxygen released from the bubbles, the soluble sulfides should be oxidated by the oxygen resulting in the decline in soluble sulfides. Based on these results, the enhancement induced by the NBs may not caused by the addition of oxygen, but the nano bubbles with long lifetime, which will contribute to the dispersion further to increase the dissolution of sulfides (s) by decreasing the particle sizes. Therefore, with the sulfide concentration lower than the toxic concentration, the more soluble sulfide may be benefit for the anaerobic digestion.

4.3.3 Effect of S concentrations

Methanogenic bacteria are known to require reduced sulphur, e.g. sulfide or cysteine, as a source of a sulfur for growth (Bryant et al., 1971). It is well known that methanogens possess a unique sulphur-rich cofactor, coenzyme M (2-mercaptoethanesulfonic acid), used in methane formation. Furthermore, methanogenic bacteria contain, in addition to coenzyme M, a large

number of iron-sulfur proteins, which presumably take part in the electron transport (Merchant et al., 2012).

The observations made above indicate that the consumed sulphide is used for two main purposes: primarily to produce sulphur compounds taking part in the energy production and also to form sulphur-containing amino acids, proteins, etc. (i.e., as a general sulphur source for new building blocks required for growth). (Ronnow et al., 1981).

While, sulfate and sulfer-containing organic compounds can be reduced to sulfide by the microbes under anaerobic conditions, and superfluous sulfide may hinder the anaerobic digestion process by two major inhibitory mechanisms. The organic acids competition caused by the sulfate-reducing bacteria is the main inhibition. Moreover, sulphide also have toxic effect on microorganisms. Free unionized hydrogen sulphide can pass through the cell membrane and react with the cell components when above certain concentration. Hydrogen sulphide level in anaerobic environments affects the microbial production of S-containing proteins and their related metabolic mechanisms (Bragg et al., 2006).

(1) Methane production

L-cystaine was chosen as the sulfur source. Cysteine has been reported to have the properties of stabilizing oxidation-reduction potential, affecting catalytic activity, and making posttranslational modifications of some proteins. For example, it can lower the redox potential, scavenge oxygen, stimulate the reduction of iron (III) oxides by Geobacter sulfurreducens, affect biohydrogen production, mediate electron transfer between different guilds, and act as nitrogen source supplier. Data showed that endogenous CH_4 production was lower in the absence of cysteine (Fig. 4-6), and CH_4 production increased with the increasing concentrations of cysteine. While, the increment in methane production was the most obvious for the groups without cysteine addition.

(2) VFAs variation

Same as the last section, the dominant product of VFAs is acetic acid, with the amount of over 90% (Fig. 4-7). The maximum accumulation was found with the cysteine concentration of 3 mM in the IDM and INBM groups, which illustrated that the degradation rate of VFAs to CH_4. Zhuang et al. (2017) investigated the ability of cysteine for acceleration of propionate degradation, demonstrating that at an appropriate concentration, cysteine might function as an electron carrier to stimulate syntrophic propionate oxidization and CH_4 production, which can be the evidence for the deceased VFAs accumulation under higher cysteine concentration (6

mM). The stimulatory effect of air NBs on methanogenic VFAs degradation under low cysteine concentration was more apparent than the effects under higher concentrations.

(3) Fe speciation

Rare studies focus on the effect of cysteine for the speciation of trace metals. The variation of cysteine concentration affects the transformation from soluble fraction to solid phase. The soluble Fe fractions dominated the Fe speciation in the absence of cysteine (Fig. 4-8), while the addition of cysteine lead to decreased soluble fractions, instead, more sulfide and residual fractions, which can be resulted from the formation of precipitation of FeS (s). With the increment in cysteine concentration, these two fractions trended to take larger percentage.

Under lower cysteine concentrations, the NBs showed a trend to transform more soluble fractions into solid, which can be explained by the faster mass transfer. The sulfide and residual fractions in the groups with NBs were lower than the groups without NBs.

(4) Soluble sulfide

Soluble sulfides are the products of anaerobic reduction of cysteine. At the nontoxic concentration, the sufficient sulfide content is favor to the synthesis of proteins such as the essential S-containing enzymes. The higher soluble sulfide content in the groups with NBs was obtained than that without NBs, which is also consistent with the lower content in the solid phase (Fig. 4-9).

4.4 Summary

The stimulation for methane production by air NBs was more obvious under lower iron or cysteine concentrations with an increment of 30.78% without iron addition and 32.45% without cysteine supply, respectively. The methane production was inhibited at high Fe concentration, while the more obvious inhibition was obtained in NB group.

The particle distribution analysis indicated that the bubbles may combine with the particles, which resulted in a decreased zeta potential. While the ORP before and after introduction of NBs did not change obviously indicating the oxygen included in the NBs may not the main reason for the higher methane yield. For the metal speciation analysis, the increase in Fe concentrations lead to an increase in adsorbed fractions, and the existence of NBs enhanced this increment. The Fe bioavailability was mainly influenced by the Fe/S ratio. The effect of nano bubbles (stimulation or inhibition) depends on different conditions. Under optimal condition, the nano bubbles will benefit the microbial growth and methane yield.

Table 4-1 Operating conditions required in the Stover sequential extraction method

Fraction	Extracting agent	Extraction conditions	
		Shaking time	Temperature
S1. Exchangeable	30 mL KNO_3 (1 M, pH=7)	16 h	20ºC
S2. Sorbed	48 mL KF (0.5 M, pH=6.5)	16 h	20ºC
S3. Organically bound	48 mL $Na_4P_2O_4$ (0.1 M)	16 h	20ºC
S4. Carbonates	48 mL EDTA (0.1 M, pH=6.5)	2×8 h	20ºC
S5. Sulfides	30 mL HNO_3 (1 M)	16 h	20ºC
S6. Residual	10 mL distilled water and 10 mL aqua regia (HCl/HNO_3, 3:1)	30 min	Digester

Table 4-2 Summary of experimental design

Groups	Conditions					Indexes	Objectives
	Air nano bubbles	Medium components	Methanogens	Fe concentration (μM)	Cysteine concentration (mM)		
Medium with air nano bubbles (NBM)	+	+	−	50	3	Gaseous: H_2, CO_2 Liquid: TOC Fe speciation (only for medium) Bubble size distribution Zeta potential Oxidation-reduction potential (ORP) pH	Evaluate the effect of air nano bubbles for the physicochemical properties of medium and water
Medium without air nano bubbles (DM)	−	+	−	50	3		
Air nano bubble water (NBW)	+	−	−	0	0		
Distilled water without nano bubbles (DW)	−	−	−	0	0		
Isolated medium with air nano bubbles (INBM)	+	+	+	0, 50, 100	0, 3, 6	Gaseous: H_2, CO_2 & CH_4 Liquid: VFAs Solid: TS & VS, Metal speciation, Soluble sulfide	Investigate the effect of air nano bubbles on bioconversion under varied Fe concentration
Isolated medium without air nano bubbles (IDM)	−	+	+	0, 50, 100	0, 3, 6		

Table 4-3 The particle size distribution and zeta potential and oxidation and reduction potential of different groups

Groups	Mean particle size (nm)	Total particle number (/mL)	Zeta potential (mV)	ORP	pH	DO
NBW-initial	112.9±40.5	$2.92\times10^{7}\pm8.80\times10^{5}$	-26.91±3.10	-	-	-
DM-initial	105.6±6.9	$8.45\times10^{8}\pm6.19\times10^{7}$	-31.80±1.90	-320	7.60	5.01
NBM-initial	121.8±3.9	$7.86\times10^{8}\pm3.29\times10^{7}$	-26.62±2.05	-312	7.45	5.15
NBW-final	135.3±20.2	$8.59\times10^{6}\pm4.57\times10^{5}$	-23.79±4.12	-	-	-
DM-final	150.0±3.5	$1.13\times10^{9}\pm3.44\times10^{7}$	-25.73±0.32	-344	7.69	4.46
NBM-final	171.0±22.8	$1.60\times10^{8}\pm3.80\times10^{7}$	-21.36±0.45	-330	7.48	4.53

*NBW-initial – distilled water with nano bubbles at the beginning of the experiment;
DM-initial – pure medium without nano bubbles at the beginning of the experiment;
NBM-initial – pure medium with nano bubbles at the beginning of the experiment;
NBW-final – distilled water with nano bubbles at the end of the experiment;
DM-final – pure medium without nano bubbles at the end of the experiment;
NBM-final – pure medium with nano bubbles at the end of the experiement.

(a)

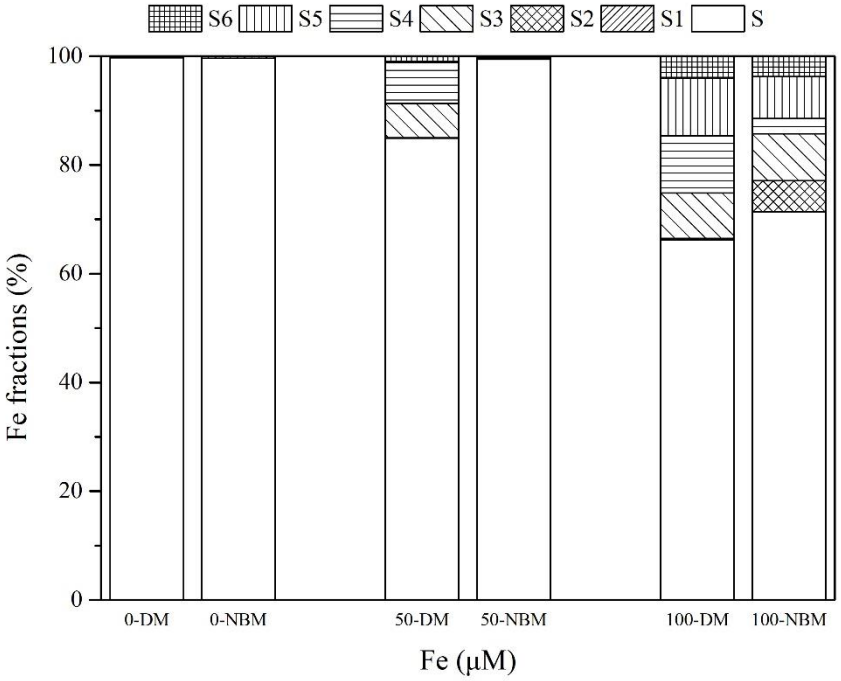

(b)

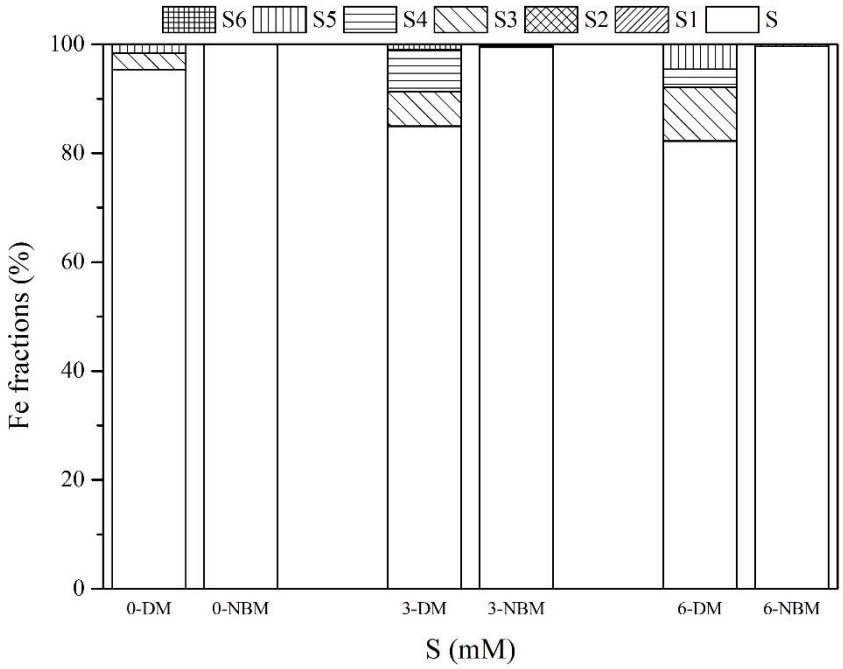

Fig. 4-1 The Fe speciation under different concentrations for DM (pure medium without nano bubbles) and NBM (pure medium with nano bubbles) groups (a) with varied Fe concentrations; (b) with varied cysteine concentrations.

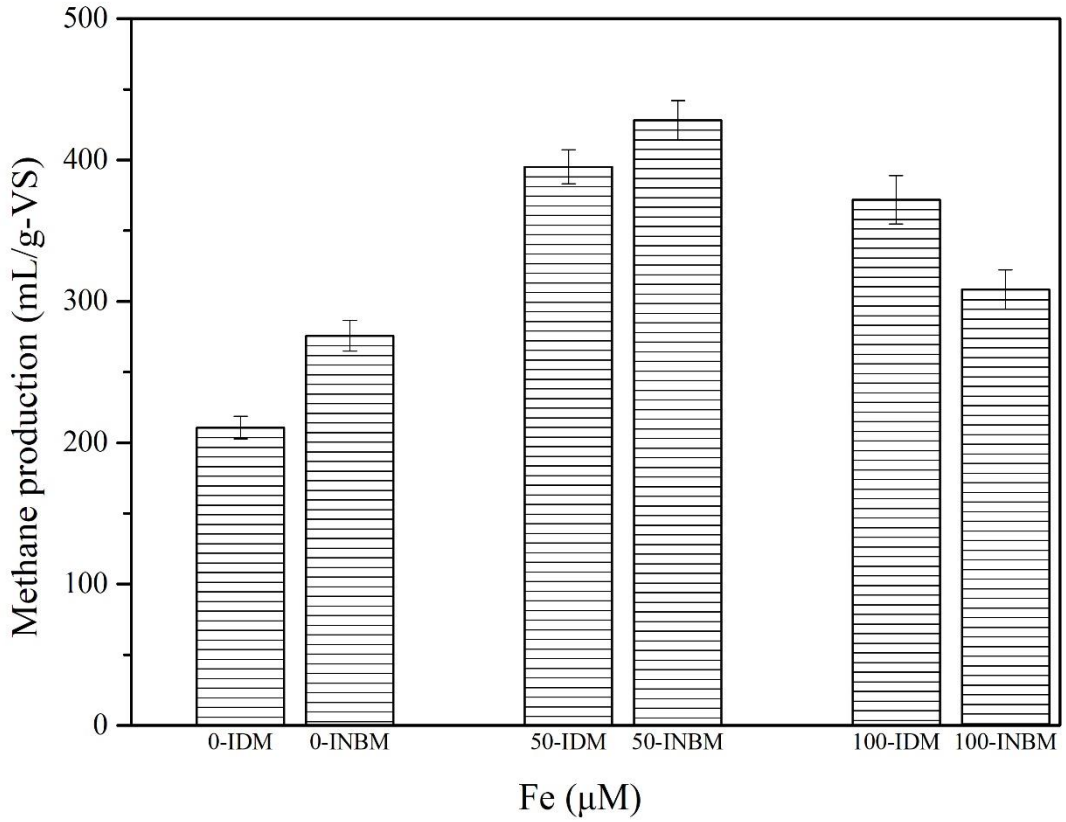

Fig. 4-2 The accumulated methane production under different Fe concentration for IDM (isolated medium without nano bubbles) and INBM (isolated medium with nano bubbles) groups.

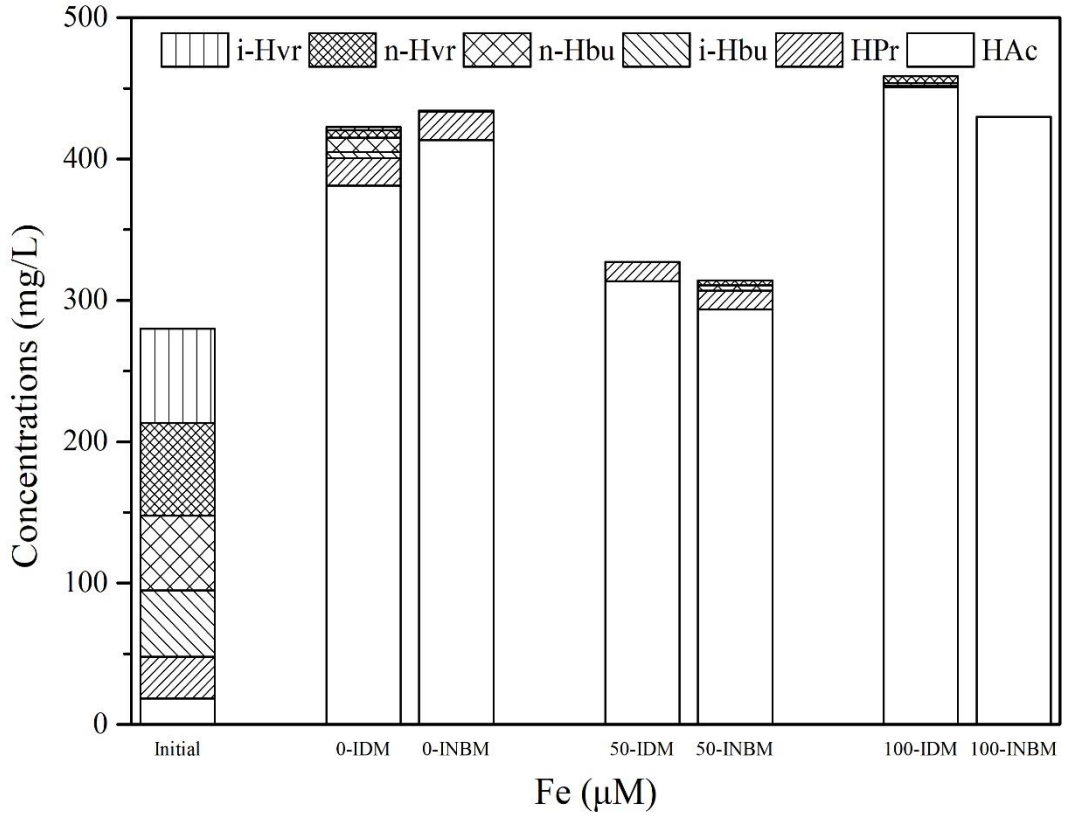

Fig. 4-3 The VFAs variation under different Fe concentration for IDM (isolated medium without nano bubbles) and INBM (isolated medium with nano bubbles) groups.

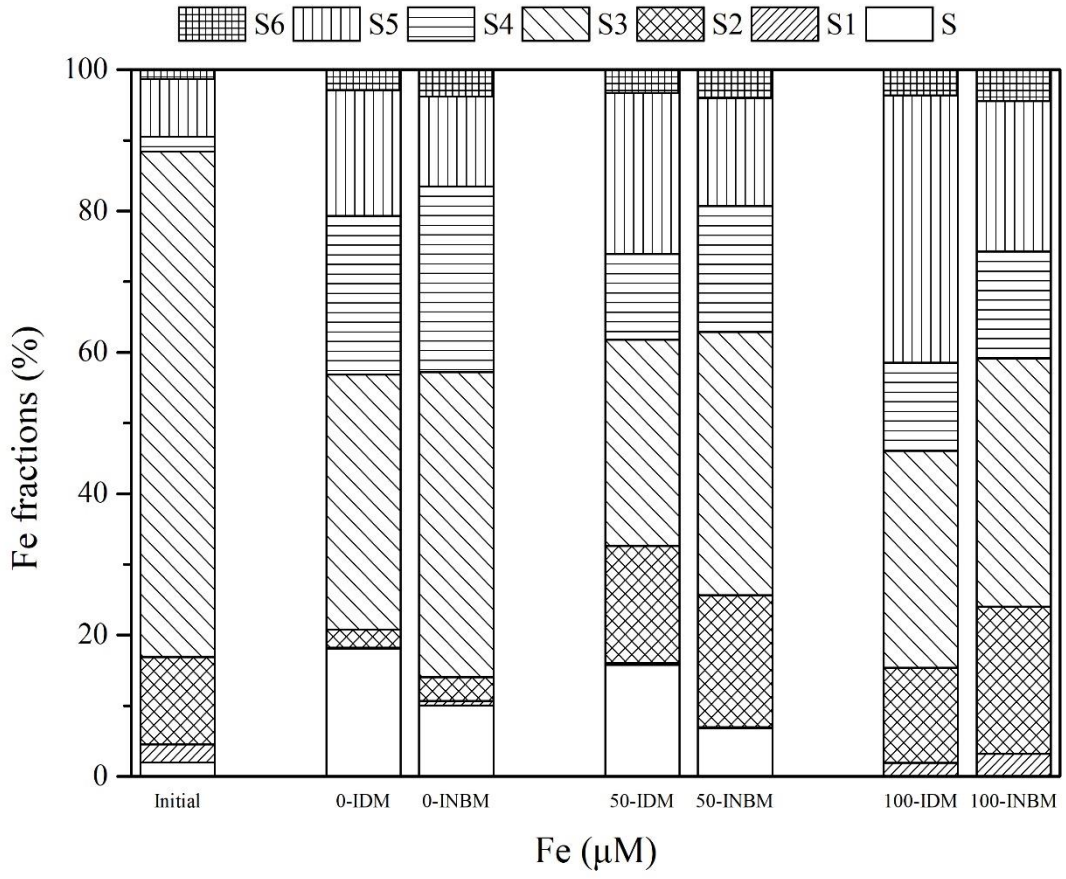

Fig. 4-4 The Fe speciation under different Fe concentration for IDM (isolated medium without nano bubbles) and INBM (isolated medium with nano bubbles) groups. (S-soluble fraction, S1- exchangeable fraction, S2- adsorbed fraction, S3 organically bounded fraction, S4-Carbonate fraction, S5-sulfide fraction, S6-residual)

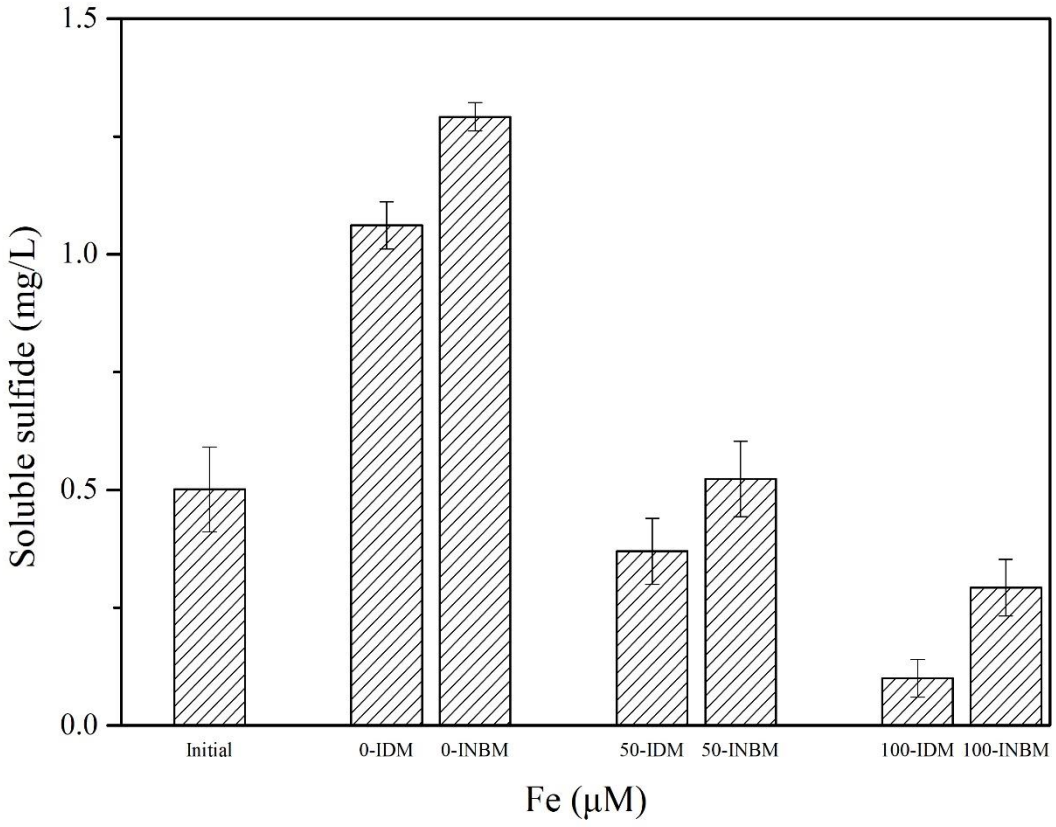

Fig. 4-5 The soluble sulfide concentration under different Fe concentration for IDM (isolated medium without nano bubbles) and INBM (isolated medium with nano bubbles) groups.

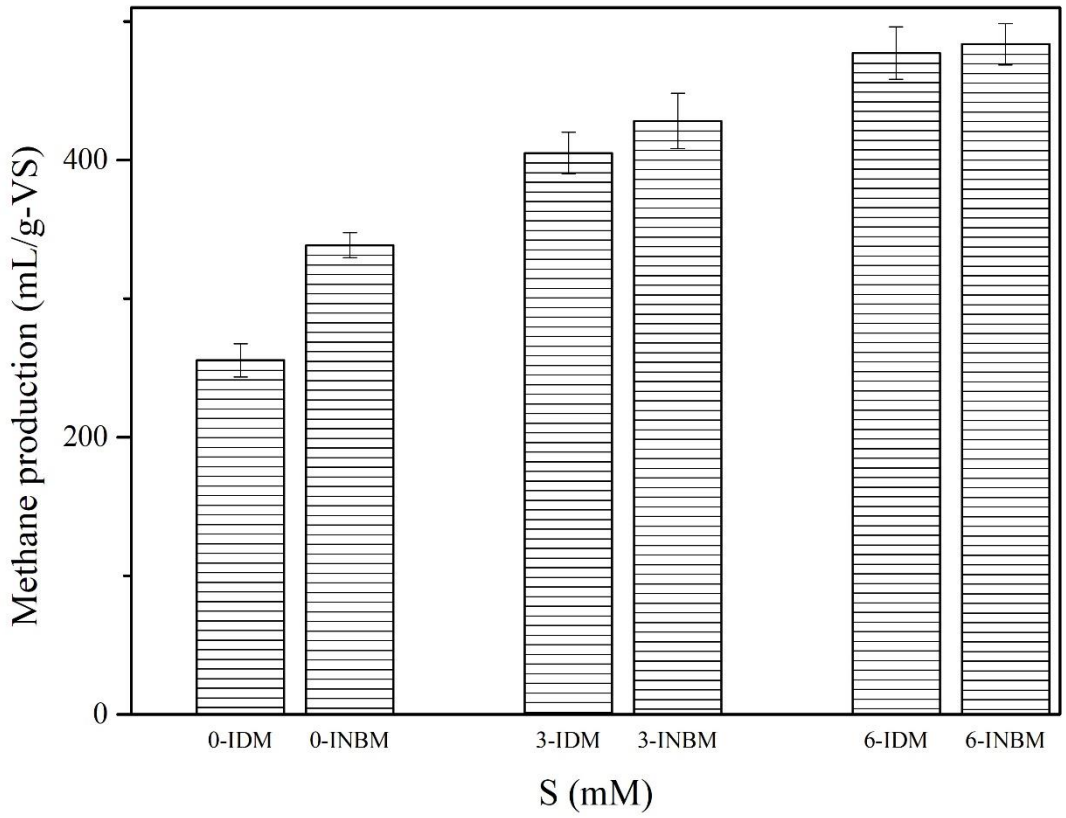

Fig. 4-6 The methane production under different cysteine concentration for IDM (isolated medium without nano bubbles) and INBM (isolated medium with nano bubbles) groups.

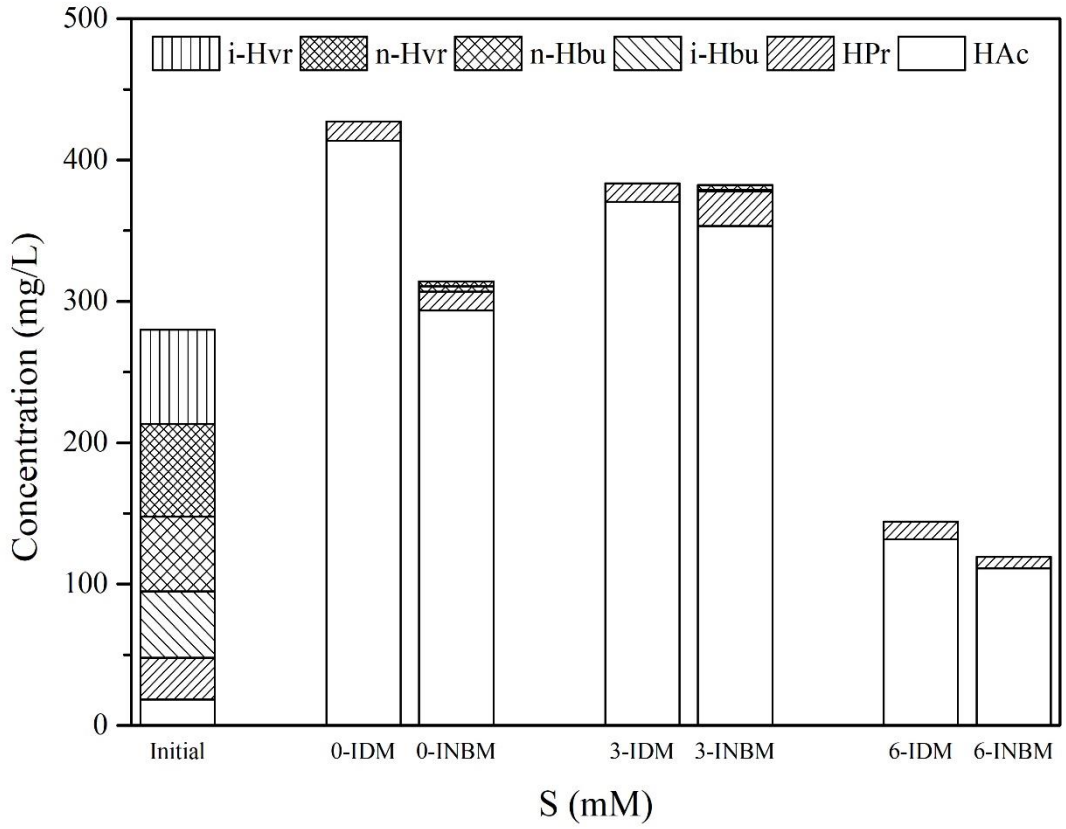

Fig. 4-7 The VFAs variation under different cysteine concentration for IDM (isolated medium without nano bubbles) and INBM (isolated medium with nano bubbles) groups.

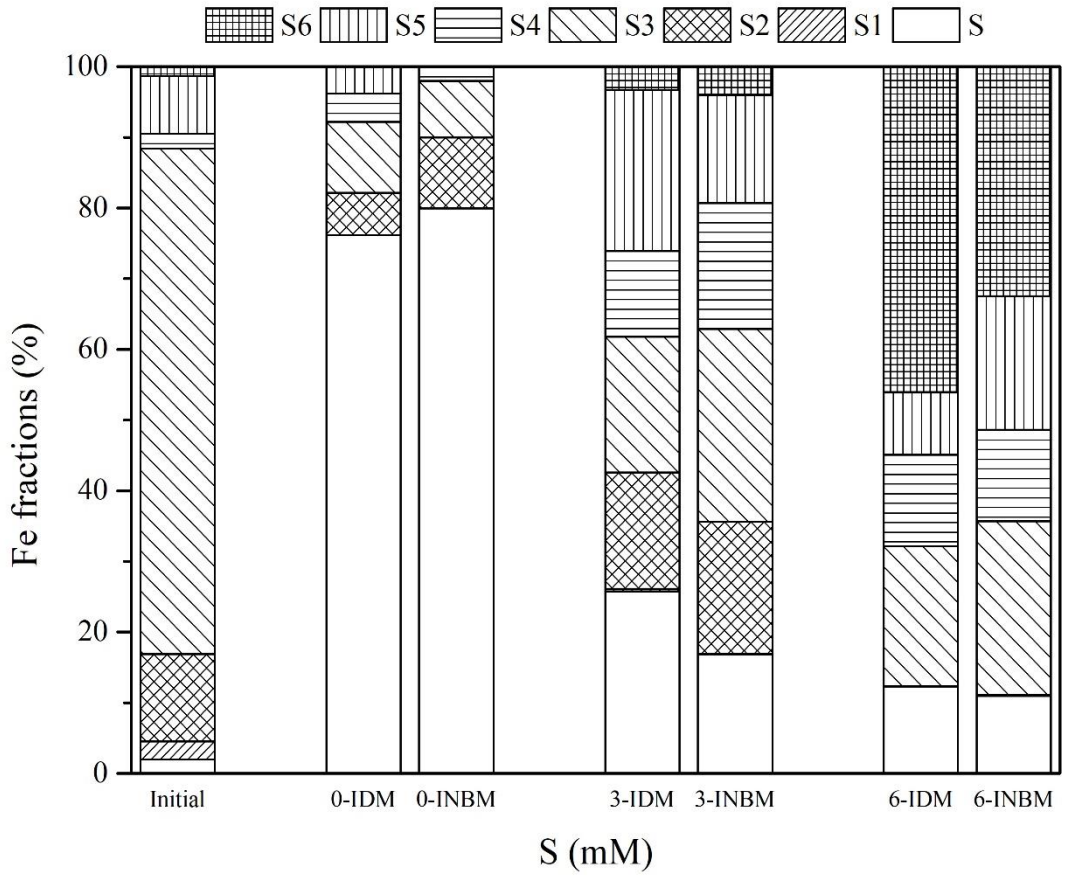

Fig. 4-8 The Fe speciation under different cysteine concentration for IDM (isolated medium without nano bubbles) and INBM (isolated medium with nano bubbles) groups. (S-soluble fraction, S1- exchangeable fraction, S2- adsorbed fraction, S3-organically bounded fraction, S4-Carbonate fraction, S5-sulfide fraction, S6-residual)

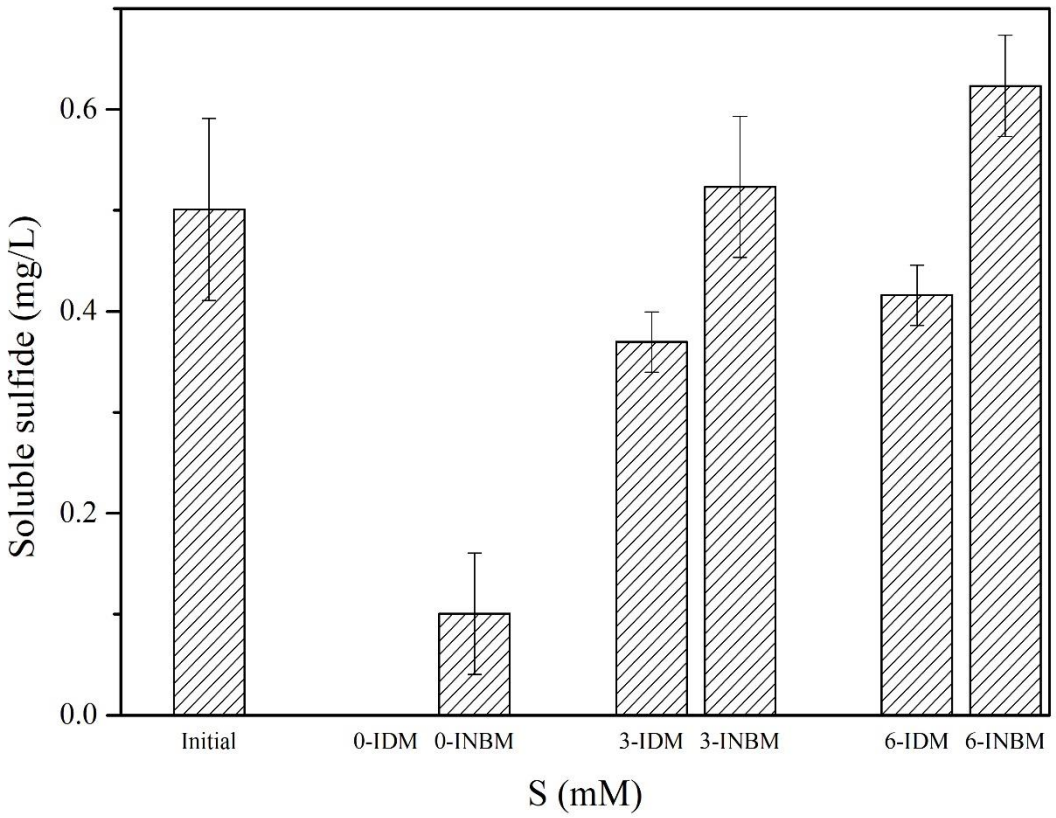

Fig. 4-9 The soluble sulfide concentration under different cysteine concentration for IDM (isolated medium without nano bubbles) and INBM (isolated medium with nano bubbles) groups.

Chapter 5 Conclusions and Future research

The conversion of CO_2 to other valuable carbonic compound is one of the effective way to alleviate the greenhouse effect in the world. Unlike the chemical procedure, which employs the costly catalysts, such as Ru, Pb, Rh, etc, under the high pressure or temperature condition, the bioconversion of CO_2 by hydrogenotrophic methanogens can realize the transformation from CO_2 to biofuel (CH_4) under a mild condition with a lower cost. However, the mass transfer of hydrogen, and the low biomass growth rate remain as the hurdles for this procedure. In order to convert CO_2 to CH_4 more effectively, the micro-nano bubbles was utilized to overcome the limitations, considering the specific characteristics, larger interfacial area, long retention time and surface charge. Though a series of experiments including feasibility, mechanism and influencing factors researches, the following conclusions were obtained.

5.1 Enhanced bioconversion of hydrogen and carbon dioxide to methane using a micro-nano sparger system

The bioconversion performance for the stirred tank reactors equipped with a common micro sparger and a micro-nano sparger were compared. The conclusions were as follows:

1) The enhanced bioconversion of H_2 and CO_2 to CH_4 was realized with the higher maximum methane evolution rate of 171.4 mmol/L_R/d by using the MNS than that of 136.1 mmol/L_R/d by the CMS.

2) The MNSR also displayed superior biomass growth with a higher specific growth rate (0.15 d^{-1}).

3) The VFAs accumulation was not detectable in MNSR.

4) Higher gas-liquid mass transfer was achieved in the MNSR (12.95 h^{-1}) than that in the CMSR (6.60 h^{-1}).

5) A higher energy-product ratio and economic analysis indicates that MNS has applicable potential for improvement of CO_2 and H_2 conversion into CH_4 in large-scale plants.

5.2 Enhanced bioconversion of H_2 and CO_2 to methane by pre-loaded bulk nano bubbles (NBs) via improving trace metal bioavailability

The effect of nano bubbles (NBs) on the hydrogenotrophic methanogens was investigated by preparing liquid medium with or without H_2/CO_2 mixture nano bubbles. The conclusions

were drawn as follows:

1) Methane yield was enhanced by the pre-supplementation of NBs in the liquid with the maximum daily production of 264. 53 mL/g-VS, while 238.05 mL/g-VS without NBs.

2) The higher coenzyme F_{420} content was improved by 1.23 fold via the addition of nano bubbles.

3) The intracellular Fe contents (1159.53±20.34 μg/g-VS) in INBM group were higher than the distilled water (IDM) group (1035.28±12.01 μg/g-VS), which can be the evidence for the higher coenzyme content.

4) For the metal speciation analysis, the higher percentage of acid soluble and exchangeable fraction, while lower percentage of organic matter and sulfide fractions in the NBW group were achieved than the DW group.

5) The micro-nano bubbles may enhanced the mass transfer and bioavailability of trace metals. This study indicated that the bulk nano bubbles have the potential for the enhancement of methane production or other microbial stimulation.

5.3 The effect of air nano bubbles on iron bioavailability in anaerobic digester under varied iron and sulfur concentrations

The effect of air NBs on bioconversion of H_2 and CO_2 to CH_4 was investigated under different initial iron and cysteine (sulfur source) concentrations. Following conclusions were obtained:

1) The stimulation for methane production by air NBs was more obvious under moderate iron or cysteine concentrations (maximum methane yield at 50 μM (395.14 mL/g-VS for control group, 428.17 mL/g-VS for NB group, respectively).

2) The methane production was inhibited at high Fe concentration (decreased to 308.32 mL/g-VS in NB group and 371.90 mL/g-VS in control group, respectively)., while the more obvious inhibition was obtained in NB group.

3) The particle distribution analysis indicated that the bubbles may combine with the particles, which resulted in a decreased zeta potential. While the ORP before and after introduction of NBs did not change obviously indicating the oxygen included in the NBs may not the main reason for the higher methane yield.

4) For the metal speciation analysis, the increase in Fe concentrations lead to an increase in adsorbed fractions, and the existence of NBs enhanced this increment.

5.4 Future research

In this study, the effect of micro-nano bubbles on the bioconversion of H_2 and CO_2 to CH_4 was investigated. Although we proposed a hypothesis that the nano bubbles may improve the trace metal bioavailability and biouptake, the deeper research should be explored in the future research.

1) The experiments utilizing pure strains of methanogens may be necessary to better understand the effect of nano bubbles on the methanogens.

2) The interaction of particles, microorganisms and bubbles should be investigated by utilizing the AFM or some other effective methods.

3) The changes for the metabolism of methanogens with the existence of nano bubbles should be revealed in a micro scale.

4) The long-term influence of air nano bubbles on the methanogens is worth to be found out by conducting an experiment continuously supply the air nano bubbles.

5) The application of nano bubbles for other anaerobic microorganisms and the degradation of hard degradable substance.

References

Agarwal A, Ng WJ, Liu Y. (2011). Principle and applications of microbubble and nanobubble technology for water treatment. Chemosphere, 84(9), 1175-1180.

APHA. (2005). Standard Methods for the Examination of Water and Wastewater. 21st ed., American Public Health Association/American Water Work Association/Water Environment Federation, Washington, DC.

Aronu UE, Svendsen HF, Hoff KA. (2010). Investigation of amine amino acid salts for caorbon dioxide absorption. Int. J. Greenh. Gas. Con., 4(5), 771-775.

Bassani I, Kougias PG, Treu L, Angelidaki I. (2015). Biogas upgrading via hydrogenotrophic methanogenesis in two-stage continuous stirred tank reactors at mesophilic and thermophilic conditions. Environ. Sci. Technol., 49, 12585–12593.

Bassani I, Kougias PG, Angelidaki I. (2016). In-situ biogas upgrading in thermophilic granular UASB reactor: key factors affecting the hydrogen mass transfer rate. Bioresour. Technol., 221, 485–491.

Bassani I, Kougias PG, Treu L, Porte H, Campanaro S, Angelidaki I. (2017). Optimization of hydrogen dispersion in thermophilic up-flow reactors for ex situ biogas upgrading. Bioresour. Technol., 234, 310-319.

Bashiri G, Rehan MA, Greenwood RD, Dickson JMJ, Baker NE. (2010). Metabolic Engineering of Cofactor F_{420} Production in *Mycobacterium smegmatis*. Plos one, 5(12), 1-10.

Bredwell MD, Telgenhoff MD, Barnard S, Worden RM. (1997). Effect of surfactants on carbon monoxide fermentations by *Butyribacterium methylotrophicum*. Appl. Biochem. Biotechnol., 63–65, 637–647.

Bryant MP, Tzeng SF, Robinson IM, Joyner AE. (1971). Nutrient requirements of methanogenic bacteria. Adv. in Chem., 105, 23-40.

Benemann JR. (2000). Hydrogen production by microalgae. J Appl Phycol, 12, 291–300.

Bonacker LG, Baudner S, Moerschel E. (1993). Properties of the two isoenzymes of methyl-coenzyme M reductase in Methanobacterium thermoautotrophicum. Eur J Biochem, 217, 587–95.

Botheju D, Samarakoon G, Chen C, Bakke R. (2010). An experimental study on the effecs of oxygen in bio-gasification; Part 2, in proceedings of the International Conference on Spain, March, 2010.

Bragg JG, Thomas D, Baudouin-Cornu P. (2006). Variation among species in proteomic sulphur content is related to environmental conditions, Proc. R. Soc. B. Bio. Sci., 273, 1293-1300.

Bredwell MD, Srivastava P, Worden RM. (1999). Reactor design issues for synthesis-gas fermentations. Biotechnol. Prog. 15, 834–844.

Brooks KP, Hu J, Zhu H, Kee RJ. (2007). Methanation of carbon dioxide by hydrogen reduction using the Sabatier process in microchannel reactors. Chem. Eng. Sci., 62, 1161–70.

Burkhardt M & Busch G. (2013). Methanation of hydrogen and carbon dioxide. Appl. Energy, 111, 74-79.

Cavicchioli R. (2011). Archaea – timeline of the third domain. Nat. Rev. Microbiol., 9, 51–61.

Chang IS, Kim BH, Lovitt RW. (2001). Effect of CO partial pressure on cell-recycled continuous CO fermentation by *Eubacterium limosum KIST612*. Process Biochem. 37, 411–421.

Chen Y, Cheng JJ, Creamer KS. (2008a). Inhibition of anaerobic digestion process: a review. Bioresour. Technol., 99, 4044–4064.

Chen SD, Lee KS, Lo YC, Chen WM, Wu JF, Lin CY, Chang JS. (2008b). Batch and continuous biohydrogen production from starch hydrolysate by Clostridium species. Int. J. Hydrogen Energy, 33, 1803–1812.

Chu L, Zhang X, Li X, Yang F. (2005). Simultanious removal of organic substances and nitrogen using a membrane bioreactor seeded with anaerobic granular sludge under oxygen-limited conditions. Desalination, 172, 271-280.

Cord-Ruwisch R, Lovley DR, Schink B. (1998). Growth of *Geobacter sulfurreducens* with acetate in syntrophic cooperation with hydrogen-oxidizing anaerobic partners. Appl. Environ. Microbiol. 64, 2232-2236.

de Filippis P, Borgianni C, Paolucci M. (2004). Prediction of syngas quality for two-stage gasification of selected waste feedstocks. Waste Manage., 24, 633–639.

de Poorter LMI, Geerts WJ, Keltjens JT. (2007). Coupling of Methanothermobacter thermautotrophicus methane formation and growth in fed-batch and continuous cultures under different H_2 gassing regimens. Appl. Environ. Microbiol., 73, 740–749.

Deppenmeier U. (2002). The unique biochemistry of methanogenesis. Prog Nucleic Acid Res Mol Biol, 71, 223–283.

Diaz I, Perez C, Alfaro N, Fdz-Polanco F. (2015). A feasibility study on the bioconversion of CO_2 and H_2 to biomethane by gas sparging through polymeric membranes. Bioresour. Technol., 185, 246-253.

DiMarco AA, Bobik TA, and Wolfe RS. (1990). Unusual coenzymes of methanogenesis. Annu. Rev. Biochem. 59, 355-394.

Dixon AJ, Dhanaliwala AH, Chen JL, Hossack JA. (2013). Enhanced intracellular delivery of a model drug using microbubbles produced by a microfluidic devices. Ultrasound Med. Biol., 39(7), 1267-1276.

Endo A, Srithongouthai S, Nashiki H, Teshiba I, Iwasaki T, Hama D, Tsutsumi H. (2008). DO increasing effects of a microscopic bubble generating system in a fish farm. Mar. Pollut. Bull., 57(1), 78–85.

Fan X, Tao D, Honake R, Luo R. (2010). Nanobubble generation and its applications in froth flotation (part II): fundamental study and theoretical analysis. Min. Sci. Technol. (China), 20(2),159–177.

Ferry JG. (2011). Fundamentals of methanogenic pathways that are key to the biomethanation of complex biomass. Curr. Opin. Biotechnol., 22(3), 351-357.

Francisco GJ, Chakama A, Feng X. (2010). Separation of carbon dioxide from nitrogen using diethanolamine-impergnated poly(vinyl alcohol) membranes. Sep. Purif. Technol., 75, 205-213.

Frigon JC & Guiot SR. (1995). Impact of liquid-to-gas hydrogen mass transfer on substrate conversion efficiency of an upflow anaerobic sludge bed and filter reactor. Enzyme Microb. Technol., 17, 1080-1086.

Ghirardi ML, Zhang L, Lee JW. (2000). Microalgae: a green source of renewable H_2. Trends Biotechnol., 18, 506–11.

GIO. (2015) National greenhouse gas inventory report of JAPAN.

Ginter MO, Grobicki AM. (1995). Analysis of anaerobic sludge containing heavy metals: A novel technique. Water Res., 29(12), 2780-2784.

Gonzalez-Gil G, Kleerebezem R, Lettinga G. (1999). Effects of nickel and cobalt on kinetics of methanol conversion by methanogenic sludge as assessed by on-line CH_4 monitoring. Appl. Environ. Microbiol., 65, 1789-1793.

Guiot SR, Cimpoia R, Carayon G. (2011). Potential of wastewater-treating anaerobic granules for biomethanation of synthesis gas. Environ. Sci. Technol., 45, 2006–2012.

Gustavsson J, Yekta SS, Karlsson A, Skyllberg U, Svensson BH. (2013). Potential bioavailability and chemical forms of Co and Ni in the biogas process-An evaluation based on sequential and acid volatile sulfide extractions. Eng. Life Sci., 13(6), 572-579.

Haarhoff J, Edzwald JK. (2001). Modelling of floc-bubble aggregate rise rates in dissolved air flotation. Water Sci. Technol., 43(8), 175–184.

Hao L, He P, Lu F, Shao L, and Zhu M. (2009). Regulating the hydrolysis of organic waste by micro-aeration and effluent recirculation. Waste Manage., 29, 2042-2050.

Hoekman SK, Broch A, Robbins C, Purcell R. (2009). CO_2 recycling by reaction with renewably-generated hydrogen. Int. J. Greenh. Gas Con., 4, 44-50.

Huang W, Huang W, Yuan T, Zhao Z, Cai W, Zhang Z, Lei Z, Feng C. (2016). Volatile fatty acids (VFAs) production from swine manure through short-term dry anaerobic digestion and its separation from nitrogen and phosphorus resources in the digestate. Water Res., 90, 344-353.

Jee HS, Nishio N, Nagai S. (1988a). Methane production from hydrogen and carbon dioxide by *Methanobacterium thermoautotrophicum* cells fixed on hollow fibers. Biotechnol Lett, 10, 243–248.

Jee HS, Nishio N, Nagai S. (1988b). Continuous methane production from hydrogen and carbon dioxide by *Methanobacterium thermoautotrophicum* in a fixed-bed reactor. J Ferment Technol, 66, 235–238.

Jeffrey A, Donald L, Willian H. (1990). Increased oxygen transfer in a yeast fermentation using a microbubble dispersion. Appl. Biochem. Biotechnol., 24, 470-484.

Jiang Y, Zhang Y, Banks C, Heaven S, Longhurst P. (2017). Investigation of the impact of trace elements on anaerobic volatile fatty acid degradation using a fractional factorial experimental design. Water Res., 125, 458-465.

Ju D, Shin J, Lee H, Kong S. (2008). Effects of pH conditions on the biological conversion of carbon dioxide to methane in a hollow-fiber membrane biofilm reactor (Hf-MBfR). Desalination, 234, 409-415.

Karakashev D, Batstone DJ, Trably E, Angelidaki I. (2006). Acetate oxidation is the dominant methanogenic pathway from acetate in the absence of *Methanosaetaceae*. Appl. Envion. Microbilo. 72, 5138-5141.

Ketheesan B, Stuckey DC. (2015). Effects of hydraulic/organic shock/transient loads in anaerobic wastewater treatment: a review. Crit. Rev. Environ. Sci. Technol., 45, 2693-2727.

Ketheesan B, Thanh PM, Stuckey DC. (2016). Iron deficiency and bioavailability in anaerobic batch and submerged membrane bioreactors (SAMBR) during organic shock loads. Bioresour. Technol., 211, 136-145.

Khuntia S, Majumder SK, Ghosh P. (2015). Quantitative prediction of generation of hydroxyl radicals from ozone microbubbles. Chem. Eng. Res. Des., 98, 231–239.

Klasson KT, Ackerson CMD, Clausen EC. (1992). Biological conversion of synthesis gas into fuels. Int. J. Hydrogen Energy 17, 281–288.

Kobayashi F, Ikeura H, Tamaki M, Hayata Y. (2010). Application of CO_2 micro- and nano-bubbles at lower pressure and room temperature to inactivate microorganisms in cut Wakegi (Allium Wakegi Araki). Southeast Asia Symposium on Quality and Safety of Fresh and Fresh-cut Produce, 875, 417-424.

Krayzelova L, Bartacek J, Diaz I, Jeison D, Volcke EIP, Jenicek P. (2015). Microaeration for hydrogen sulphide removal during anaerobic treatment: a review. Rev. Environ. Sci. Bio-Technol., 14(4), 703-725.

Kugino K, Tamaru S, Hisatomi Y, Sakaguchi T. (2016). Long-duration carbon dioxide anesthesia of fish using ultra fine (nano-scale) bubbles. Plos one, 11(4), 1-9.

Kurata K, Taniguchi T, Fukunaga T, Matsuda J, Higaki H. (2008). Development of a compact microbubble generator and its usefulness for three-dimensional osteoblastic cell culture. Colloids Surf. A, 2, 166–177.

Lake DL, Kirk PWW, Lester JN. (1985). The effects of anaerobic digestion on heavy metal distribution in sewage sludge. Water Pollut. Control, 84, 549–558.

Lam MK, Lee KT, Mohamed AR. (2012). Current status and challenges on microalgae-based carbon capture. Int. J. Greenh. Gas Con., 10, 456-469.

Lee M & Zinder SH. (1988). Hydrogen partial pressure in a thermophilic acetate-oxidizing methanogenic coculture. Appl. Environ. Microbiol., 54, 1457-1461.

van Leeuwen HP, Town RM, Buffle J, Cleven RFMJ, Davison W, Puy J, van Riemsdijk W, Sigg L. (2005). Dynamic speciation analysis and bioavailability of metals in aquatic systems. Environ. Sci. Technol., 39(22), 8545-8556.

Li H, Hu L, Xia Z. (2013). Impact of groundwater salinity on bioremediation enhanced by micro-nano bubbles. Materials, 6, 3676–3687.

Li H, Hu L, Song J, Al-Tabbaa A. (2014). Subsurface Transport Behavior of Micro-Nano Bubbles and Potential Applications for Groundwater Remediation. Int. J. Environ. Res. Public Health, 11, 473-486.

Lindahl PA & Chang B. (2001). The evolution of acetyl-CoA synthase. Orig. Life Evol. Biosph. 31, 403-434

Liu Y & Whitman WB. (2008). Metabolic, phylogenetic, and ecological diversity of the methanogenic archaea. Ann. N. Y. Acad. Sci., 1125, 171–189.

Liu K, Atiyeh HK, Stevenson BS. (2014). Continuous syngas fermentation for the production of ethanol, n-propanol and n-butanol. Bioresour. Technol. 151, 69–77.

Liu S, Oshita S, Kawabata S, Makino Y, Yoshimoto T. (2016). Identification of ROS produced by nanobubbles and their positive and negative effects on vegetable seed germination. Langmuir, 32, 11295-11302.

Ljunggren S, Eriksson JC. (1997). The lifetime of a colloid-sized gas bubble in water and the cause of the hydrophobic attraction. Colloids Surf. A, 129, 151−155.

Luo G & Angelidaki I. (2013). Co-digestion of manure and whey for in situ biogas upgrading by the addition of H_2: process performance and microbial insights. Appl. Microbiol. Biotechnol., 97, 1373–1381.

Luo G, Wang W, Angelidaki I. (2013). Anaerobic digestion for simultaneous sewage sludge treatment and CO biomethanation: Process performance and microbial ecology. Environ. Sci. Technol. 47, 10685-10693.

Ma X, Yang X, Zhang S. (2013). Study on the inhibitory effect of bayberry tannin extract on anaerobic fermentation. Appl. Mech. Mater., 361-363, 562-566.

Merchant SS & Helmann JD. (2012). Elemental economy: Microbial strategies for optimizing growth in the face of nutrient limitation. Adv. Microb. Physiol., 60, 91-210.

Miettinen T, Ralston J, Fornasiero D. (2010). The limits of fine particle flotation. Miner. Eng. 23(5), 420–437.

Mishchuk N, Ralstion J, Fornasiero D. (2006). Influence of very small bubbles on particle/bubble heterocoagulation. J. Colloid Interf. Sci., 301, 168-175.

Mudhoo A & Kumar K. (2013). Effects of heavy metals as stress factors on anaerobic digestion processes and biogas production from biomass. Int. J. Environ. Sci. Technol., 10, 1383–1398.

Muller V. (2003). Energy conservation in acetogenic bacteria. Appl. Environ. Microbiol., 69, 6345-6353.

Munasinghe PC & Khanal SK. (2010). Syngas fermentation to biofuel: evaluation of carbon monoxide mass transfer coefficient (k_La) in different reactor configurations. Biotechnol. Prog., 26, 1616–1621.

Munasinghe PC & Khanal SK. (2014). Evaluation of hydrogen and carbon monoxide mass transfer and a correlation between the myoglobin-protein bioassay and gas chromatography method for carbon monoxide determination. RSC Advances, 4(71), 37575-37581.

Nghiem LD, Manassa P, Dawson M, Fitzgerald SK. (2014). Oxygen injection into anaerobic digester for reducing hydrogen sulphide concentration in biogas. Bioresour. Technol., 173, 443-447.

Nishimura N, Kitaura S, Mimura A, Takahara Y. (1992). Cultivation of thermophilic methanogen KN-15 on hydrogen-carbon dioxide under pressurized conditions. J Ferment Bioeng, 73, 477-480.

Ortner M, Rameder M, Rachbauer L, Bochmann G, Fuchs W. (2015). Bioavailability of essential trace elements and their impact on anaerobic digestion of slaughterhouse waste. Biochem. Eng. J. 99, 107-113.

Osuna MB, van Hullebusch ED, Zandvoort MH, Iza J, Lens PN. (2004). Effect of cobalt sorption on metal fractionation in anaerobic granular sludge. J. Environ. Qual., 33, 1256-1270.

Pauss A, Andre G, Perrier M, Guiot SR. (1990). Liquid-to-gas mass transfer in anaerobic processes: inevitable transfer limitations of methane and hydrogen in the biomethanation process. Appl. Environ. Microbiol., 56, 1636-1644.

Peillex JP, Fardeau ML, Belaich JP. (1990). Growth of Methanobacterium thermoautotrophicum on hydrogen-carbon dioxide: high methane productivities in continuous culture. Biomass, 21, 315-321.

Redwood MD & Macaskie LE. (2006). A two-stage, two-organism process for biohydrogen from glucose. Int. J. Hydrogen. Energ., 31, 1514-1521.

Redwood MD, Orozco RL, Majewski AJ, Macaskie LE. (2012). Electroextractive fermentation for efficient biohydrogen production. Bioresour. Technol., 107, 166-174.

Rittmann S., Seifert A, Herwig C. (2015). Essential prerequisites for successful bioprocess development of biological CH_4 production from CO_2 and H_2. Crit. Rev. Biotechnol., 35, 141-151.

Rittmann S & Herwig C. (2012). A comprehensive and quantitative review of dark fermentative biohydrogen production. Microb. Cell Fact., 11, 115.

Rittmann S, Seifert A, Herwig C. (2012). Quantitative analysis of media dilution rate effects on *Methanothermobacter marburgensis* grown in continuous culture on H_2 and CO_2. Biomass Bioeng., 36, 293-301.

Robinson CW, Wilke CR. (1973). Oxygen absorption in stirred tanks: a correlation for ionic strength effects. Biotechnol. Bioeng., 15, 755-782.

Ronnow PH & Gunnarsson LAH. (1981). Sulfide-dependent methane productionand growth of a thermophilic methanogenic bacterium. Appl. Envirion. Microbiol., 42(4), 580-584.

Roennow PH, Gunnarsson LAH. (1982). Response of growth and methane production to limiting amounts of sulfide and ammonia in two thermophilic methanogenic bacteria. FEMS Microbiol. Lett., 14, 311-315.

Rospert S, Linder D, Ellermann J, Thauer RK. (1990). Two genetically distinct methyl-coenzyme M reductases in Methanobacterium thermoautotrophicum strain Marburg and Delta H. Eur J Biochem, 194, 871–877.

Rospert S, Boecher R, Albracht SPJ, Thauer RK. (1991). Methylcoenzyme M reductase preparations with high specific activity from hydrogen-preincubated cells of Methanobacterium thermoautotrophicum. FEBS Lett, 291, 371–375.

Rubio J, Souza ML, Smith RW. (2002). Overview of flotation as a wastewater treatment technique. Miner. Eng., 15(3), 139–155.

Sahuquillo A, López-Sánchez JF, Rubio R, Rauret G, Thomas RP, Davidson CM, Ure AM. (1999). Use of a certified reference material for extractable trace metals to assess sources of uncertainty in the BCR three-stage sequential extraction procedure. Anal. Chim. Acta, 382, 317–327.

Sayari A, Belmabkhout Y, Serna-Guerrero R. (2011). Flue gas treatment via CO_2 adsorption. Chem. Eng. J., 171, 760-774.

Seddon JRT, Lohse D, Ducker WA, Craig VSJ. (2012). A deliberation on nanobubbles at surfaces and in bulk, Chem. Phys. Chem. 13, 2179–2187.

Stover RC, Sommers LE, Silveira DJ. (1976). Evaluation of metals in wastewater sludge. J. Water Pollut. Control Fed., 48, 2165.

Szuhaj M, Ács N, Tengölics R, Bodor A, Rákhely G, Kovács KL, Bagi Z. (2016). Conversion of H_2 and CO_2 to CH_4 and acetate in fed-batch biogas reactors by mixed biogas community: a novel route for the power-to-gas concept. Biotechl Biofuels, 9, 102.

Takahashi M. (2009). Base and Technological Application of Micro-Bubble and Nano-Bubble. Mater. Integr., 22, 2–19.

Tessier A, Campbell PG, Bisson M. (1979). Sequential extraction procedure for the speciation of particulate trace metals. Anal. Chem. 51, 844–851

Thauer RK, Kaster AK, Seedorf H, Buckel W, Hedderich R. (2008). Methanogenic archaea: ecologically relevant differences in energy conservation. Nat Rev Microbiol, 6, 579–591.

Thauer RK, Kaster AK, Goenrich M, Schick M, Hiromoto T, Shima S. (2010). Hydrogenases from methanogenic archaea, nickel, a novel cofactor, and H_2 storage. Annu. Rev. Biochem., 79, 507-536.

Tsapekos P, Kougias PG, Treu L, Campanaro S, Angelidaki I. (2016). Process performance and comparative metagenomic analysis during co-digestion of manure and lignocellulosic biomass for biogas production. Appl. Energy. 185, 126–135.

Tsuge H. (2014). Characteristics of microbubbles: micro- and nanobubbles. Chapter 1.

Ure AM, Quevauviller P, Muntau H, Griepink B. (1993). Speciation of heavy metals in soils and sediments. An account of the improvement and harmonization of extraction techniques undertaken under the auspices of the BCR of the commission of the european communities. Int. J. Environ. Anal. Chem., 51, 135–151.

Ushikubo FY, Furukawa T, Nakagawa R, Enari M, Makino Y, Kawagoe Y, Shiina K, Oshita S. (2010). Evidence of the existence and the stability of nano-bubbles in water. Colloids and Surfaces A: Physicochem. Eng. Aspects, 361, 31-37.

van der Veen A, Fermoso FG, Lens PNL. (2007). Bonding form analysis of metals and sulfur fractionation in methanol-grown anaerobic granular sludge. Eng. Life Sci., 7, 480-489.

Vega JL, Clausen EC, Gaddy JL. (1989). Study of gaseous substrate fermentations-carbon monoxide conversion to acetate. 1. Batch culture. Biotechnol. Bioeng., 34(6), 774-784.

Weimer PJ & Zeikus JG. (1978). One carbon metabolism in methanogenic bacteria: cellular characterization and growth of *methanosarcina barkeri*. Arch. Microbiol., 119, 49-57.

Wilkinson KJ & Buffle J. (2004). Critical evaluation of physicochemical parameters and processes for modelling the biological uptake of trace metals in environmental (aquatic) systems. In Physicochemical Kinetics and Transport at Biointerfaces; van Leeuwen HP, Koster W, Eds; vol. 9, IUPAC Series on Analytical and Physical Chemistry of Environmental Systems; Buffle J, van Leeuwen HP, Series Eds; Wiley: Chichester, 445-533.

Wu C, Wang L, Harbottle D, Masliyah J, Xu Z. (2015). Studying bubble-particle interactions by zeta potential distribution analysis. J. Colloid Inter. Sci., 449, 399-408.

Xie L, Cui X, Huang J, Wang J, Liu Q, Zeng H. (2018). Probing the interaction mechanism between air bubbles and bitumen surfaces in aqueous media using bubble probe atomic force microscopy. Langmuir, 34, 729-738.

Xu G, Liang F, Yang Y, Hu Y, Zhang K, Liu W. (2014). An improved CO_2 separation and purification system based on cryogenic separation and distillation theory. Energies 7, 3484-3502.

Xu R, Zhang K, Liu P, Khan A, Xiong J, Tian F, Li X. (2018). A critical review on the interaction of substrate nutrient blance and microbial community structure and function in anaerobic co-digestion. Bioresour. Technol., 247, 1119-1127.

Yagi H, Yoshida F. (1975). Enhancement factor for oxygen absorption into fermentation broth. Biotechnol. Bioeng. 17, 1083–1098.

Yoon RH. (1993) Microbubble flotation. Miner. Eng. 6(6), 619–30.

Zandvoort MH, van Hullebusch ED, Fermoso FG, Lens PNL. (2006). Trace metals in anaerobic granular sludge reactors: bioavailability and dosing strategies. Eng. Life Sci., 6, 293-301.

Zayed G & Winter J. (2000). Inhibition of methane production from whey by heavy metals-protective effect of sulfide. Appl. Microbiol. Biotechnol., 53, 726–731.

Zee YY, Thiam LC, Peng WZ, Abdul RM, Chai S. (2013). Synthesis and performance of microporous inorganic membranes for CO_2 separation: a review. J. Porous Mater., 20, 1457-1475.

Zhang M, Seddon JRT. (2016). Nanobubble-nanoparticle interactions in bulk solutions. Langmuir, 32, 11280-11286.

Zhang W, Zhang L, Li A. (2015). Enhanced anaerobic digestion of food waste by trace metal elements supplementation and reduced metals dosage by green chelating agent [S, S]-EDDS via improving metals bioavailability. Water Res., 84, 266-277.

Zhang Y, Zhang Z, Suzuki K, Maekawa T. (2003). Uptake and mass balance of trace metals for methane producing bacteria. Biomass Bioenerg, 25, 427-433.

Zhang Z, Maekawa T. (1993). Kinetic study on fermentation from CO_2 and H_2 using the acclimated-methanogen in batch culture. Biomass Bioenerg., 4(6), 439-446.

Acknowledgement

I would like to express my sincere gratitude to my academic advisor, Professor Zhenya Zhang, for his guidance, encouragement during my three-year study in Tsukuba. He is an excellent example I can follow throughout my life, not only his academic level but also his attitude of life.

I would also like to thank the other academic advisor, Professor Zhongfang Lei and Professor Kazuya Shimizu, for their supervision, guidance and support during the doctoral study in Tsukuba. I also need to express my grateful to Professor Motoyashi Kobayashi for providing me the important equipments.

I also would like to express my great appreciation to my dissertation committee members, Professor Kaiqin Xu, Professor Lei, Professor Shimizu. and really appreciate their numerous suggestion, comments, and the previous time to serve as my advisory committee members.

Special appreciation is expressed to my supervisor in master's degree, Professor Chuanping Feng, for giving me the chance to pursue higher education and improve research ability at University of Tsukuba. Thanks for China Scholarship Council (CSC) for offering me the scholarship to complete my research.

During the past three years, I received lots of help from my friends and fellow students. They deserve recognition for their direct and indirect contributions to this dissertation. Here I express my heartfelt appreciation to them.

I reserve much of my appreciation for my family. This dissertation would not be completed without their love and support.

This dissertation is dedicated to the people of the world who have devoted their lives to the protection of our environment.

Appendix

1. Liu, Ye, Wang, Ying, Wen Xinlei, et al. Enhanced bioconversion of hydrogen and carbon dioxide to methane using a micro-nano sparger system: mass balance and energy consumption. RSC Advances, 2018, 8, 26488-26496.

2. Liu, Ye, Zhang, Baogang, et al. Optimization of enhanced bio-electrical reactor with electricity from microbial fuel cells for groundwater nitrate removal using response surface methodology, Environmental Technology, 2016, 37(8), 1008-1017.

3. Liu, Ye, Zhang, Baogang, et al. Research Progress in Combination of Microbial Fuel Cell and Conventional Wastewater Treatment Technology. World Science and Technology Research and Development, 2014, 36(5), 480-487.

4. Hu, Qili, **Liu, Ye**, Feng, Chuanping, et al. Predicting equilibrium time by adsorption kinetic equations and modifying Langmuir isotherm by fractal-like approach, Journal of Molecular Liquids, 2018, 268, 728-733.

5. Zhang, Baogang, **Liu, Ye**, Huang, Wenli, et al. A bibliometric analysis of research on hexavalent chromium removal from 1975 to 2012, Fresenius Environmental Bulletin, 2015, 24(12), 4834-4841.

6. Zhang, Baogang, **Liu, Ye**, Tong, Shuang, et al. Enhancement of bacterial denitrification for nitrate removal in groundwater with electrical stimulation from microbial fuel cells，Journal of Power Sources, 2014, 268, 423-429.

7. Zhang, Baogang, **Liu, Ye**, Tian, Caixing, et al. A bibliometric analysis of research on upflow anaerobic sludge blanket (UASB) from 1983 to 2012， Scientometrics, 2014, 100(1), 189-202.

8. Wang, Ying, Yin, Chenzhu, **Liu, Ye**, et al. Biomethanation of blast furnace gas using anaerobic granular sludge via addition of hydrogen, RSC Advances, 2018, 8, 26399-26406.

9. Liu, Huipeng, Zhang, Baogang, **Liu, Ye**, et al. Continuous bioelectricity generation with simultaneous sulfide and organics removals in an anaerobic baffled stacking microbial fuel cell, International Journal of Hydrogen Energy, 2015, 40, 8128-8136.

10. Ye, Zhengfang, Zhang, Baogang, **Liu, Ye**, et al. Continuous electricity generation with piggery wastewater treatment using an anaerobic baffled stacking microbial fuel cell, Desalination and water treatment, 2015, 55, 2079-2087.

11. Zhang, Baogang, Zhang, Jing, **Liu, Ye**, et al. Identification of removal principles and involved bacteria in microbial fuel cells for sulfide removal and electricity generation. International Journal of Hydrogen Energy, 2013, 38(33), 14348-14355.

12. Ye, Zhengfang, Zhang, Baogang, **Liu, Ye**, et al. A bibliometric investigation of research trends on sulfate removal. Desalination and Water Treatment, 2013, 52(31-33): 6040-6049.